NAGW-1333

INVESTIGATION AND MODIFICATION OF A COMMERCIALLY AVAILABLE TACTILE SENSOR SUITED FOR ROBOTIC APPLICATIONS

by

Carolina Creus

Rensselaer Polytechnic Institute
Electrical, Computer, and Systems Engineering Department
Troy, New York 12180-3590

August 1991

CIRSSE REPORT #100

CONTENTS

Page

LIST OF TABLES v

LIST OF FIGURES vii

ACKNOWLEDGEMENT x

ABSTRACT xi

1. INTRODUCTION AND HISTORICAL REVIEW 1

2. REVERSE ENGINEERING 5

   2.1 Electrical Description of the Tactile Array Pad 5

   2.2 Hardware Description 8

      2.2.1 Description of the Analog Board Components 11

      2.2.2 Selecting a Site in the Tactile Array Pad 11

      2.2.3 Voltage Map Circuit 12

      2.2.4 Digital Gain for the Signal's Amplification 14

3. CHARACTERISTICS OF THE TACTILE SENSOR ARRAY 16

   3.1 Experimental Setup 17

   3.2 Protecting the Tactile Pad 17

   3.3 Force Around the Tactile Pad Borders 18

   3.4 Force Measurement Interpolation 22

   3.5 Hysteresis Analysis 32

   3.6 Sensitivity Analysis 48

   3.7 Effects of an Applied Force on its Neighbors 53

4. SENSOR INTERFACE WITH THE 68HC11 EVALUATION BOARD 54

Page

4.1 Hardware Configuration 54

4.2 68HC11 EVB Port Assignment 58

4.2.1 Port B of the 68HC11 EVB 58

4.2.2 Port C of the 68HC11 EVB 58

4.2.2 Port E of the 68HC11 EVB 59

5. SOFTWARE DESCRIPTION AND SYSTEM OPERATION 60

5.1 Initialization 60

5.1.1 Power Up Initialization 60

5.1.2 SCI Initialization 60

5.1.3 A/D Converter Initialization 60

5.2 Software Location on Memory 61

5.3 Communication Software between Host and 68HC11 EVB 61

5.3.1 Host Communication Software 62

5.3.2 68HC11 EVB Communication Software 63

5.4 Software Developed to Control the Tactile Sensor 63

5.4.1 Software Developed for the 68HC11 64

5.4.1.1 Sensor Commands 64

5.4.1.1.1 tacScanAll Command 64

5.4.1.1.2 tacElementOne Command 65

5.4.1.2 A/D Converter Operation 65

5.4.2 Software Developed for the Host Computer 66

5.5 Data Acquisition Example 67

6. DISCUSSION 70

7. CONCLUSIONS 75

Page

LITERATURE CITED 77

BIBLIOGRAPHY 78

LIST OF TABLES

Page

Table 2.1 Connections From the Sensor Pad to the Analog Board 9

Table 3.1 Forces Recorded on Corner #1 of the Sensor Pad 18

Table 3.2 Forces Recorded on Corner #2 of the Sensor Pad 19

Table 3.3 Forces Recorded on Corner #3 of the Sensor Pad 20

Table 3.4 Forces Recorded on Corner #4 of the Sensor Pad 21

Table 3.5 Force Interpolation Measurements for Test Point #1.....23

Table 3.6 Force Interpolation Measurements for Test Point #2.....25

Table 3.7 Force Interpolation Measurements for Test Point #3.....27

Table 3.8 Force Interpolation Measurements for Test Point #4.....29

Table 3.9 Hysteresis Data Taken at Test Point #1 for Experiment #1..... 33

Table 3.10 Hysteresis Data Taken at Test Point #2 for Experiment #1..... 35

Table 3.11 Hysteresis Data Taken at Test Point #3 for Experiment #1..... 37

Table 3.12 Hysteresis Data Taken at Test Point #1 for Experiment #2..... 39

Table 3.13 Hysteresis Data Taken at Test Point #2 for Experiment #2..... 41

Table 3.14 Hysteresis Data Taken at Test Point #3 for Experiment #2..... 43

Table 3.15 Hysteresis Data Taken at Test Point #1 for Experiment #3..... 45

Table 3.16 Hysteresis Data Taken at Test Point #2 for Experiment #3..... 46

Table 3.17 Hysteresis Data Taken at Test Point #3 for Experiment #3..... 47

Table 4.1 Connections between Analog Board and 68HC11 EVB.....55

Table 4.2 List of Diodes on the Sensor Pad and Configuration for Port C so they can be Activated.....56

Page

Table 4.3 List of Transistors on the Sensor Pad and Configuration for Port B so they can be Activated.....57

Table 5.1 Analog Input to 8-Bit Result Translation Table.....66

LIST OF FIGURES

Page

Figure 2.1 Diagram of the Existing Sites in the Sensor Pad. 6

Figure 2.2 Optoelectronic Layout inside the Tactile Sensor Pad....7

Figure 2.3 Diode-Transistor Pair Configuration....8

Figure 2.4 Analog Board Hardware....10

Figure 2.5 Voltage Map Circuit....13

Figure 2.6 Digital Gain Chip and its Connections....14

Figure 3.1 Setup used to perform the experiments....16

Figure 3.2 Graph Corresponding to the Linear Regression Analysis Done on Test Point #1....24

Figure 3.3 Graph Corresponding to the Linear Regression Analysis Done on Test Point #2....26

Figure 3.4 Graph Corresponding to the Linear Regression Analysis Done on Test Point #3....28

Figure 3.5 Graph Corresponding to the Linear Regression Analysis Done on Test Point #4....30

Figure 3.6 Graph Corresponding to Experiment #1 using Test Point #1....34

Figure 3.7 Graph Corresponding to Experiment #1 using Test Point #2....36

Figure 3.8 Graph Corresponding to Experiment #1 using Test Point #3....38

Figure 3.9 Graph for Experiment #2 using Test Point #1....40

Page

Figure 3.10 Graph for Experiment #2 using Test Point #2..... 42

Figure 3.11 Graph for Experiment #2 using Test Point #3..... 44

Figure 3.12 Data Gathered for Experiment #3 using Test Point #1.
Runs 5, 6, and 7 of the Experiment were Plotted 46

Figure 3.13 Data gathered for Experiment #3 using Test Point #2.
Runs 2, 3, and 4 of the Experiment were Plotted 47

Figure 3.14 Data Gathered for Experiment #3 using Test Point #3.
Runs 2, 3, and 4 of the Experiment were Plotted. 48

Figure 3.15 Contour Plot of the Sensor Pad Showing an Applied
Diagonal Force. 50

Figure 3.16 Mesh Plot of the Sensor Pad Showing an Applied
Diagonal Force 50

Figure 3.17 Contour Plot of the Sensor Pad Showing a Circular Object
Pressed Against the Left Side of the Pad. 51

Figure 3.18 Mesh Plot of the Sensor Pad Showing a Circular Object
Pressed Against the Left Side of the Pad. 51

Figure 3.19 Contour Plot of the Sensor Pad Showing a Circular Object
Pressed Against the Right Side of the Pad. 52

Figure 3.20 Mesh Plot of the Sensor Pad After a Circular Object Pressed
Against the Right Side of the Pad 52

Figure 4.1 Hardware Configuration for the Tactile Sensing System 54

Figure 5.1 Host - Slave Software Configuration 62

Page

Figure 5.2 Contour Plot of the Sensor Pad Before a Circular Force is Applied....68
Figure 5.3 Mesh Plot of the Sensor Pad Before a Circular Force is Applied....68
Figure 5.4 Contour Plot of the Sensor Pad After a Circular Force is Applied....69
Figure 5.5 Mesh Plot of the Sensor Pad After a Circular Force is Applied....69

ACKNOWLEDGEMENT

I would like to express my gratitude to my thesis advisor, Dr. Robert Kelley, for his advice and guidance during the course of my research. I would also like to thank Brian Romansky, Jodi Tsai, and all the people that were there to answer my questions whenever I needed help.

Next, I want to thank my family and friends for their love and support this past year. I would like to specially thank my fiancé, Jose A. Faria, for all his help while I was finishing up this project. Finally, I would like to thank the GEM Consortium for awarding me a fellowship that allowed me to pursue this Master's degree.

ABSTRACT

The main purpose of this thesis is to explore active (dynamic) tactile sensing using a commercially available tactile array sensor. This task requires the redesign of the sensor interface and a full understanding of the old sensor hardware implementation. There were different stages to this research; the first stage involved the reverse engineering of the old tactile sensor. The second stage had to do with the exploration of the characteristics and behavior of the tactile sensor pad. The next stage dealt with the redesign of the sensor interface using the knowledge gained from the previous two stages. Finally, in the last stage, software to control the tactile sensor was developed to aid in the data acquisition process.

CHAPTER 1

INTRODUCTION AND HISTORICAL REVIEW

Many robotic tasks are attempted without sensing, thereby assuming a simplified and static world. An example could be the typical "pick and place" task of an assembly line, where the origin and destination of the object is known. As you may already know, this scenario is not very realistic. The robotic systems of the future need the ability to use sensory feedback to understand their environment. That is why sensor research is needed.

Most of the research in object recognition has been in the computer vision area. However, sometimes it is very hard to determine the characteristics of an object by just using one type of sensor. An interesting approach is to be able to supplement the visual information by another type of sensory input. This input could be a tactile sensor, which is the topic of this thesis. By adding this type of sensor, the vision information could be combined with the tactile sensor readings to produce a more robust and error free description of the objects in the environment.

While adding a tactile sensor to a robotic system can potentially produce more accurate results, it will probably add more complexity to the system. This complexity lies in how to integrate all the sensor components, and how to control and coordinate them at the same time.

There are several types of tactile sensors: piezoresistive, magnetic and electromagnetic, capacitive, electro-optic, and ferro-electric polymer sensors [1]. The piezoresistive sensors are based on materials or elements whose electrical conductivity varies as pressure is applied. Magnetic and

electromagnetic sensors use changes in their internal magnetic moment, changes in the mechanical forces applied to or by it, or changes in its physical length to sense objects in its surroundings. The next type, capacitive sensors, use capacitance changes to sense forces. Electro-optic sensors, on the other hand, rely on the modulation of a light source by the mechanical deformation of a flexible material. Lastly, ferro-electric polymer sensors use their piezoelectric and pyroelectric properties to sense applied forces.

The tactile sensor that is the subject of this thesis, falls into the electro-optic category. This category is divided into two subclasses: Total Internal Reflection (TIR), and Non-TIR [2]. The underlying principle of operation of the TIR sensors is the frustration of total internal reflection within a planar or curved waveguide caused by contact of an elastomeric membrane against the waveguide surface. The tactile sensor used in this research falls into the second subclass. In this type of sensor, the deflection of elements protruding from a touch surface (an elastomer) reduces the light transmitted to detectors by physically blocking the light. This deflection is measured and then processed by a control system in order to be converted to a signal appropriate for the system.

While raw data acquisition from the tactile sensor takes a reasonable amount of time, the conversion from deflection readings to force readings would take too long to be performed concurrently by the same microprocessor. Therefore, the solution lies in leaving the data processing part to a host computer, and only use the controlling microprocessor to perform the data acquisition.

The previous reasoning is the motivation for this research. A sensor manufactured by the Lord Corporation is used as the subject of investigation of this project. The primary advantage of this type of sensor is that a high degree of mechanical isolation could be maintained between the sensor surface and the transduction elements, thereby permitting the sensor to be very rugged [3]. One of the drawbacks of this sensor is that the shear force at each individual site can not be measured unless a special module is attached [3].

The tactile array sensor was studied and modified by replacing its original microprocessor and leaving the data processing part to a host computer. This task was accomplished by first reverse engineering the tactile sensor array, and determining which parts of the tactile sensor would still be useful after modifications to the hardware were done. Also, the characteristics and properties of this sensor were studied and a formula to convert the existing output of the sensing system, a voltage, into a force reflecting the state of the sensor was derived. Next, a new interface using the 68HC11 EVB was designed in order to use any of the Sun workstations as a host computer. Finally, software following the guidelines of the functionality implemented by the old tactile sensor was developed.

The contents of this thesis are structured such that the chronological order of the tasks is observed. Chapter 2 discusses the inner workings of the tactile array sensor and the analog board that was part of the original design. Also some issues that were encountered while studying the analog board are explained.

Chapter 3 is devoted to the investigation of the characteristics of the tactile sensor array. Four major issues are addressed at this stage. The first issue is whether some force reading could be interpolated from the sensor output and, if it was possible, how it could be done. Secondly, the hysteresis effects on the output readings are explored. Next, the issue of tactile pad sensitivity is addressed. Finally, the effects of an applied force at the surrounding neighbors of a chosen point are investigated.

The hardware interface between the 68HC11 board and the tactile sensor board is discussed in Chapter 4. In Chapter 5, the software written to control the tactile sensor is explained. Chapter 6 gives a discussion of the information and data gathered during the course of this research. Finally, Chapter 7 ends this thesis with closing remarks, and suggestions for future uses of this tactile sensor.

CHAPTER 2

REVERSE ENGINEERING

The tactile sensor, which is the subject of this research, is the LTS-200 manufactured by Lord Corporation. This sensor incorporates two forms of tactile sensing, but only one was kept after the original sensor was modified; this form of sensing is the tactile array sensor. The other form of tactile sensing was a gross load sensor and, as a result of not being able to take apart the tactile pad, it could not be incorporated into the modified sensor. Nevertheless, even if the tactile pad could be opened up, there was no guarantee that the pad could be put back together and still function properly.

2.1 Electrical Description of the Tactile Array Pad

The tactile array sensor is composed of sensitive sites embedded in an elastomeric touch surface. The sites are organized as a 10 x 16 orthogonal array with 0.071 inches between sites, as shown in Figure 2.1. In Figure 2.2, the overall internal configuration of the sensor pad is presented. Each site is composed of an emitter and a detector, as is shown in Figure 2.3. The emitter is a diode, which produces a light of a certain intensity that is proportional to the voltage through the diode. The detector is a phototransistor that receives the light emitted by the diode and amplifies it by the current gain of the phototransistor. Usually this type of configuration is used in applications where greater sensitivity is required.

16	32	48	64	80	96	112	128	144	160
15	31	47	63	79	95	111	127	143	159
14	30	46	62	78	94	110	126	142	158
13	29	45	61	77	93	109	125	141	157
12	28	44	60	76	92	108	124	140	156
11	27	43	59	75	91	107	123	139	155
10	26	42	58	74	90	106	122	138	154
9	25	41	57	73	89	105	121	137	153
8	24	40	56	72	88	104	120	136	152
7	23	39	55	71	87	103	119	135	151
6	22	38	54	70	86	102	118	134	150
5	21	37	53	69	85	101	117	133	149
4	20	36	52	68	84	100	116	132	148
3	19	35	51	67	83	99	115	131	147
2	18	34	50	66	82	98	114	130	146
1	17	33	49	65	81	97	113	129	145

Rows

Columns

Figure 2.1 Diagram of the Existing Sites in the Sensor Pad.

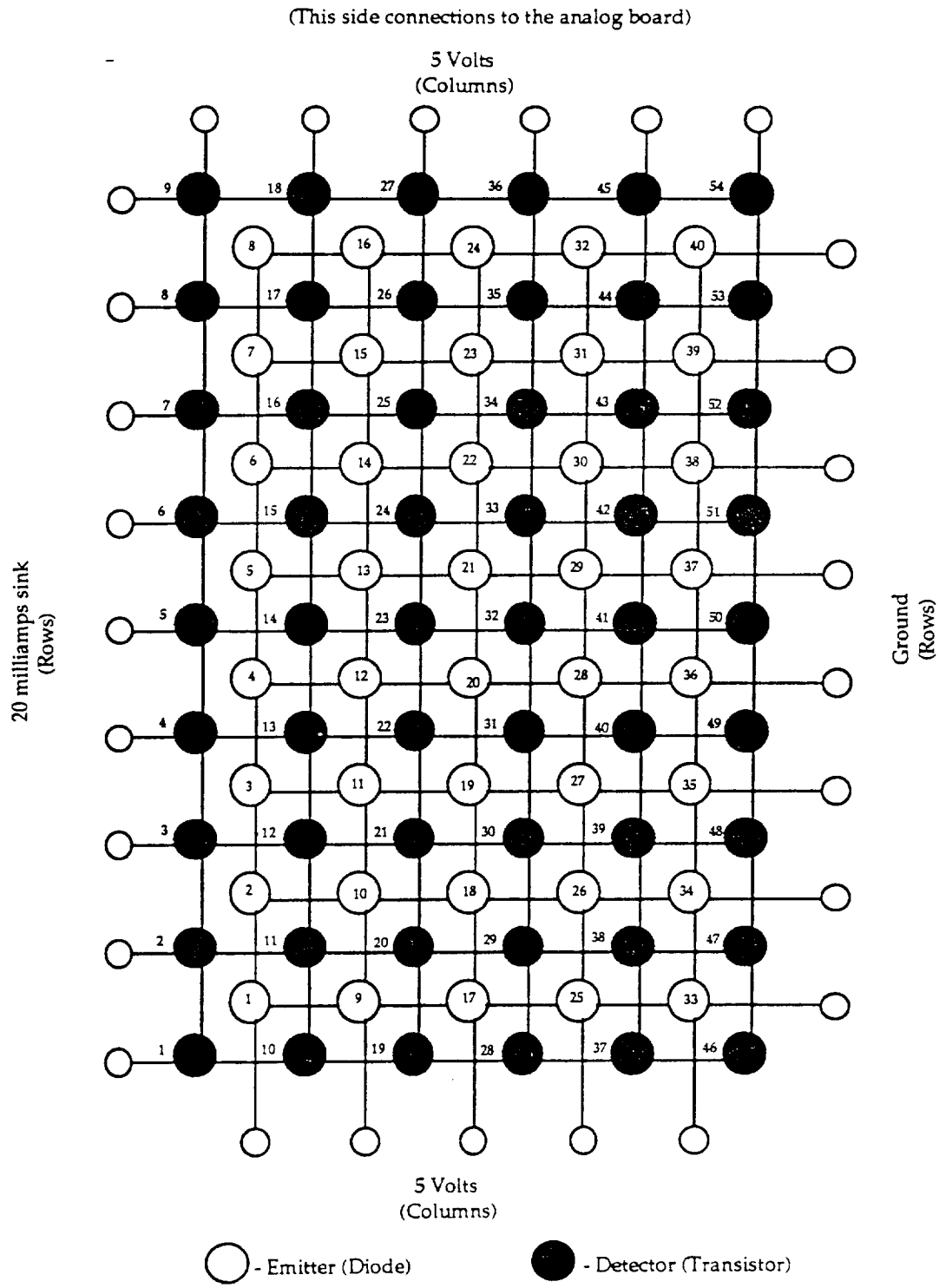

Figure 2.2 Optoelectronic Layout inside the Tactile Sensor Pad

Each site, using the previously described configuration, monitors the deflection of the small portion of the elastomeric touch surface it occupies. The result from this action is a voltage, which could be translated into an applied force. There are 40 diodes and 54 emitters on the tactile pad, which configured in the previously described fashion, produce 160 sensible sites. The location of these sites was previously shown in Figure 2.1.

2.2 Hardware Description

The first task to be accomplished was to produce schematics for the tactile sensor hardware. This need arose based on the fact that no hardware diagrams were part of the original documentation provided with the Lord Corporation tactile sensor.

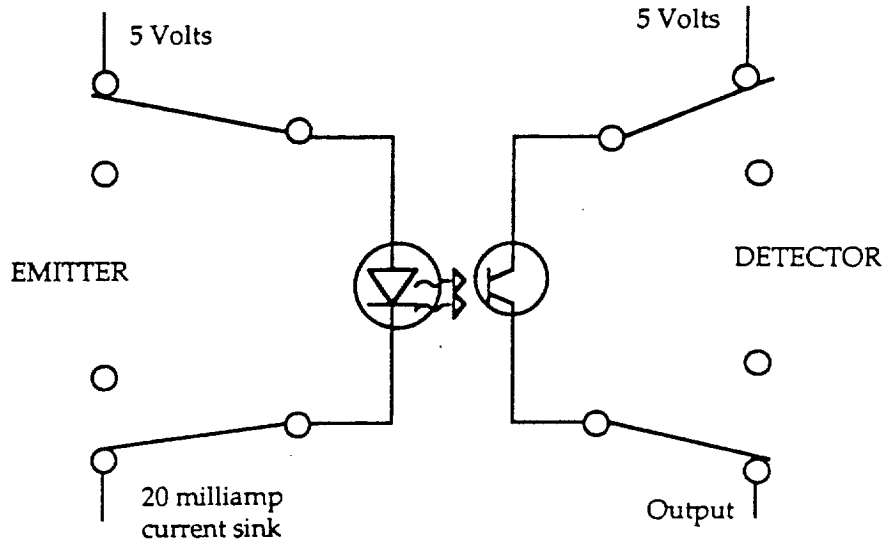

Figure 2.3 Diode-Transistor Pair Configuration

Table 2.1 Connections From the Sensor Pad to the Analog Board

Connector Pin #	Signal Name	Signal Definition	Chip number	Chip label	Component
13	+GEX	Voltage Supply	4057	U15	transistor
14	R9-D	emitter	4057	U15	transistor
15	R8-D	emitter	4057	U15	transistor
16	R7-D	emitter	4057	U15	transistor
17	R6-D	emitter	4057	U15	transistor
18	R5-D	emitter	4057	U15	transistor
19	R4-D	emitter	4057	U15	transistor
20	R3-D	emitter	4057	U15	transistor
21	R2-D	emitter	4057	U15	transistor
22	R1-D	emitter	4057	U15	transistor
23	C6+D	collector	4051	U14	transistor
24	C5+D	collector	4051	U14	transistor
25	C4+D	collector	4051	U14	transistor
26	C3+D	collector	4051	U14	transistor
27	C2+D	collector	4051	U14	transistor
28	C1+D	collector	4051	U14	transistor
29	R8-E	cathode	4051	U18	diode
30	R7-E	cathode	4051	U18	diode
31	R6-E	cathode	4051	U18	diode
32	R5-E	cathode	4051	U18	diode
33	R4-E	cathode	4051	U18	diode
34	R3-E	cathode	4051	U18	diode
35	R2-E	cathode	4051	U18	diode
36	R1-E	cathode	4051	U18	diode
37	C5+E	Anode	4051	U19	diode
38	C4+E	Anode	4051	U19	diode
39	C3+E	Anode	4051	U19	diode
40	C2+E	Anode	4051	U19	diode
41	C1+E	Anode	4051	U19	diode

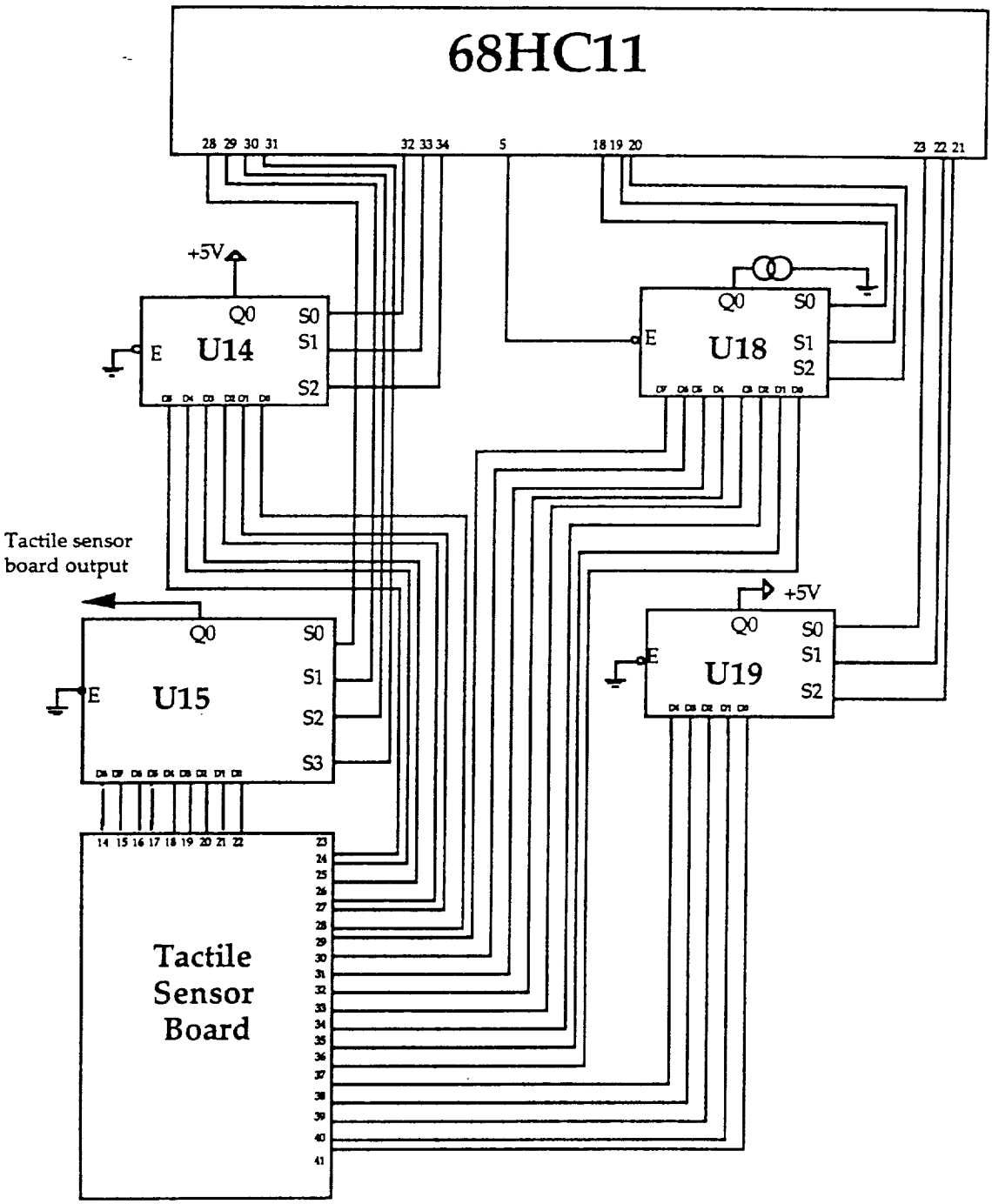

Figure 2.4 Analog Board Hardware

The hardware for the original sensor was composed of two boards: the first one contained the analog circuitry and the other one contained the digital circuitry. Since one of the objectives of this research is to replace the 6502 microprocessor of the original sensor with a 68HC11 microprocessor, it was decided not to use the digital board at all and only concentrate on how the analog board worked.

2.2.1 Description of the Analog Board Components

In Figure 2.4, devices belonging to the analog board are shown. These 4 devices are labeled as U14, U15, U18, and U19. All of them are analog multiplexers: U14, U18, and U19 are 8 channel analog multiplexers, and U15 is a 16 channel analog multiplexer. The function of these devices is to activate the diodes (U18 and U19) and transistors (U14 and U15) inside the sensor pad.

The other relevant component located on the analog board is U17, the digital gain chip. This device has as an input the voltage generated when a diode and a transitor are activated inside the sensor pad. Inside this device, the gain of the signal is increased by 32.

2.2.2 Selecting a Site in the Tactile Array Pad

The analog board contains the appropriate circuitry which takes a reading from one of 160 sites (Figure 2.1), and converts that into a voltage which could be later be transformed into a force measurement. There are

certain steps that have to be followed to select a given site in the tactile array. First, determine the appropriate diode and transistor pair corresponding to the desired site by looking at Figure 2.1. Then, find the corresponding row and column in the optoelectronic layout using Figure 2.2. After this, using Table 2.1, get the corresponding number for the connection with the tactile sensor pad. Finally, select those connections on the multiplexers shown on Figure 2.4. The multiplexers labeled as U15 and U14 correspond to the activation of the transistors. U18 and U19 correspond to the selection of a particular diode. After selecting the desired diode-transistor pair, a deflection for the desired site could be measured. This deflection is output in the form of a voltage, which is later fed to the voltage map circuit, so the A/D converter inside the 68HC11 EVB could be used.

2.2.3 Voltage Map Circuit

Before the voltage coming from the tactile sensor is fed to the 68HC11 EVB, there is some signal amplification that takes place within the analog board. The resulting amplification yields an output of a +12V to -12V range. In the original board, further processing of this signal took place. The voltage was mapped into a 0V to 5V range by using some combination of op-amps and switches. Instead of using their scheme, which is practically impossible to trace in the analog board, I decided to design my own voltage map circuit. In my scheme, I used a buffer op-amp which is directly connected to a 10 kΩ potentiometer. This potentiometer is used to adjust the gain of the circuit. The other side of the potentiometer is connected to

another 10 kΩ potentiometer which is used to adjust the offset of the output signal. The resulting output from this circuit yields the desired voltage range of 0V to 5V. Before this signal is connected to the input of the A/D, a noninverting op-amp is used to lower the loading effects caused when the connection between the 68HC11 EVB and this circuit are made. This voltage range of 0V to 5V is needed so the A/D converter supplied within the 68HC11 EVB can be used.

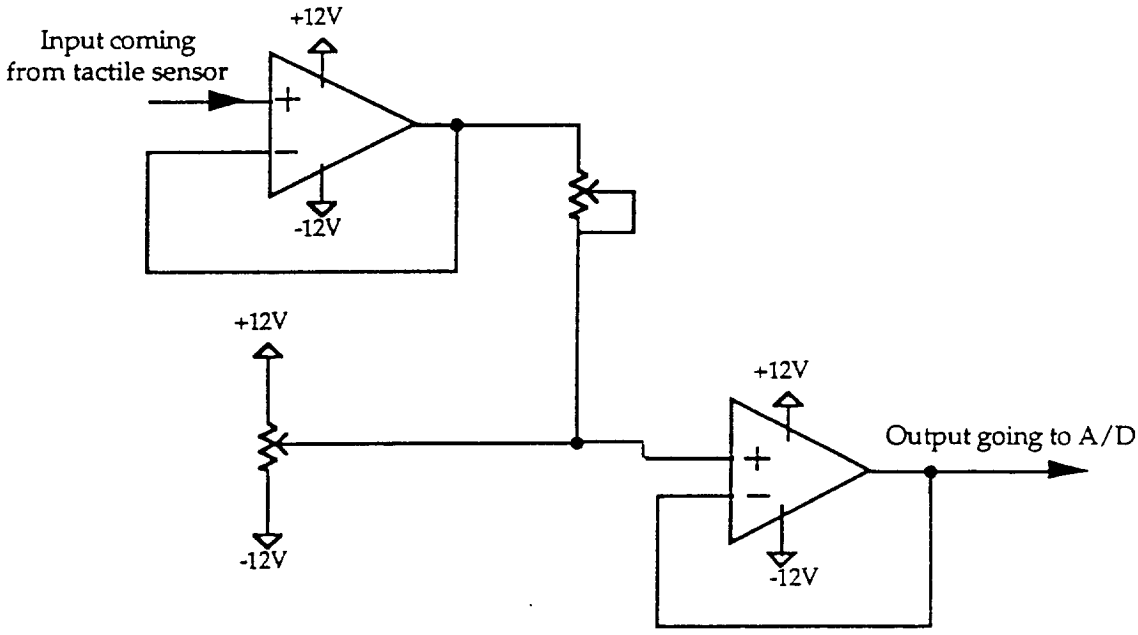

Figure 2.5 Voltage Map Circuit

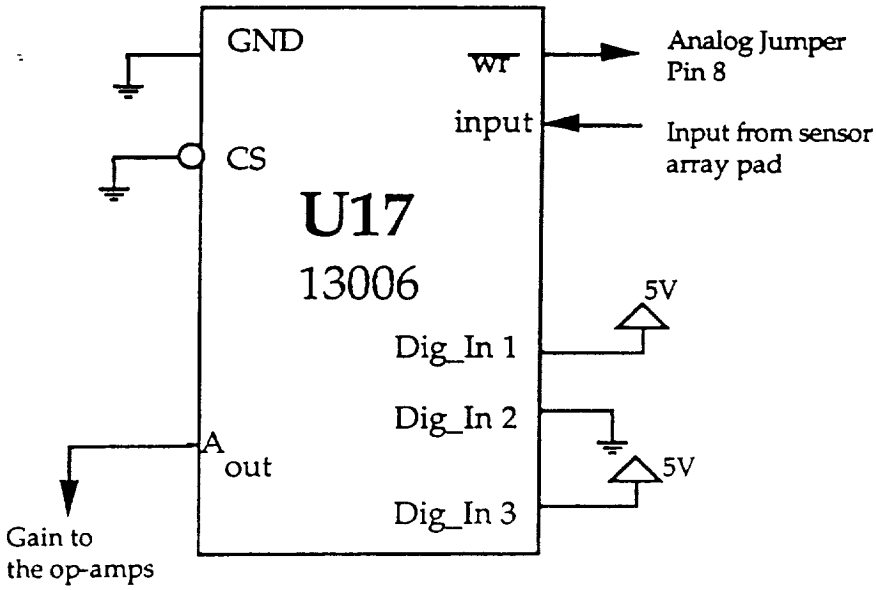

Figure 2.6 Digital Gain Chip and its Connections

2.2.4 Digital Gain for the Signal's Amplification

The analog board uses a digital gain chip in order to adjust the gain of the op-amps by means of a microprocessor. The input to this device is the signal coming from the sensor pad. At the stage where this signal enters this gain chip, it has already gone through several stages of manipulation. A detailed description of this amplification is very difficult to trace on the analog board; therefore, only the digital gain chip is shown in this thesis.

After some experiments, I decided to preset this gain to a value where the tactile array sensor will be most sensitive. The other choices in gains will yield readings only after enormous pressures are applied to the sensor. Taking into consideration that a large applied force can damage the diode-transistor pair at each site, I decided on a choice of gain (32) that will detect an

applied force within a safe range of applied pressures. In the next chapter, I will explain in detail how the safe force range was chosen.

CHAPTER 3

CHARACTERISTICS OF THE TACTILE SENSOR ARRAY

There were four major issues that had to be investigated when experiments to observe the behavior of the tactile sensor were done. The first issue is how the output voltage of the tactile sensor could be mapped into a force that could accurately represent the load on a specific site of the sensor. The second issue deals with the effect of hysteresis on the tactile pad, and how that affects the precision of the force measurements. The question of how sensitive is the tactile pad, and how precise are its results is the subject of the third issue tackled at this time. Finally, the fourth issue explores the effect on the surrounding neighbors when a force is applied to a given site.

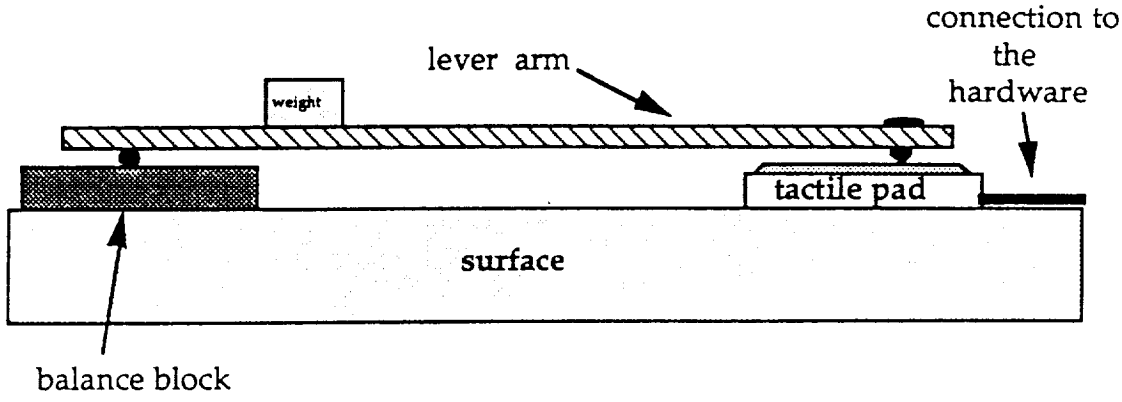

Figure 3.1 Setup used to perform the experiments

3.1 Experimental Setup

Measurements throughout the tactile pad were taken using the setup shown in Figure 3.1. This setup consists of a lever arm and a balance block. A set of weights was used to apply different forces to each site of the tactile sensor.

3.2 Protecting the Tactile Pad

In the course of the experiments, some deterioration of the tactile pad was observed. It seemed that as more continuous pressure was exerted on a point, some physical deformation was occurring to the pad. This effect is highly undesirable for two reasons: first, if deformation occurs, the force readings would not be very accurate, and second, there is no other tactile pad available if the current one ceases to function.

There were several approaches taken to alleviate this problem. The first step taken was to file the object used to apply pressure on the pad, in this case a nail, until a rounder end point was obtained. While this approach relieved some of the symptoms of deformation, it still did not completely eliminate the problem. The tactile pad is made of an elastomeric material, very rubber like, so I decided that by covering the pad with a similar material, the original characteristics of the sensor will not be lost. A typical rubber balloon seemed to be the obvious choice. It seemed to work very well, and as far as I can see there shouldn't be any difference on the measurement results with and without the balloon covering the sensor. The only problem with

using a balloon is that every couple of weeks it needs to be replaced due to wear and tear.

3.3 Force Around the Tactile Pad Borders

Several sets of measurements were taken at each one of the corners of the tactile sensor. Tables 3.1, 3.2, 3.3, and 3.4 show the results of this experiment. The experiment consisted of applying a constant force at a point, and then immediately recording the voltage reading.

Table 3.1 Forces Recorded on Corner #1 of the Sensor Pad

Distance (cm)	Voltage (Volts)	Actual Force (N)	Approximated Force (N)
9.5	8.74	0.08	0.07
9	7.54	0.11	0.11
8.5	6.05	0.15	0.16
8	3.56	0.19	0.24
7.5	0.73	0.23	0.34
7	0.76	0.26	0.33
6.5	-1.79	0.30	0.42
6	-2.23	0.34	0.43
5.5	-2.45	0.38	0.44
5	-2.60	0.41	0.45
4.5	-2.85	0.45	0.46
4	-3.28	0.49	0.47
3.5	-3.46	0.53	0.48
3	-3.62	0.57	0.48
2.5	-3.71	0.60	0.48
2	-3.79	0.64	0.49

Diode: 1 Transistor: 1 Mass Used: 100 g

Table 3.2 Forces Recorded on Corner #2 of the Sensor Pad

Distance (cm)	Voltage (Volts)	Actual Force (N)	Approximated Force (N)
10	9.93	0.02	0.03
9.5	8.87	0.04	0.06
9	6.56	0.06	0.14
8.5	4.66	0.08	0.20
8	2.98	0.09	0.26
7.5	1.34	0.11	0.32
7	0.31	0.13	0.35
6.5	-0.49	0.15	0.38
6	-1.04	0.17	0.40
5.5	-1.41	0.19	0.41
5	-1.75	0.21	0.42
4.5	-1.93	0.23	0.42
4	-2.12	0.25	0.43
3.5	-2.25	0.26	0.44
3	-2.37	0.28	0.44
2.5	-2.52	0.30	0.44
2	-2.66	0.32	0.45
1.5	-2.87	0.34	0.46
1	-2.98	0.36	0.46
0.5	-3.16	0.38	0.47

Diode: 8 Transistor: 9 Mass used: 50g

Table 3.3 Forces Recorded on Corner #3 of the Sensor Pad

Distance (cm)	Voltage (Volts)	Actual Force (N)	Approximated Force (N)
9	8.80	0.06	0.07
8.5	5.71	0.08	0.17
8	3.60	0.09	0.24
7.5	2.02	0.11	0.29
7	1.01	0.13	0.33
6.5	0.49	0.15	0.34
6	0.25	0.17	0.35
5.5	0.10	0.19	0.36
5	0.02	0.21	0.36
4.5	-0.04	0.23	0.36
4	-0.07	0.25	0.36
3.5	-0.14	0.26	0.36
3	-0.34	0.28	0.37
2.5	-0.41	0.30	0.37
2	-0.55	0.32	0.38
1.5	-0.64	0.34	0.38
1	-0.73	0.36	0.38

Diode: 40 Transistor: 54 Mass used: 50g

Table 3.4 Forces Recorded on Corner #4 of the Sensor Pad

Distance (cm)	Voltage (Volts)	Actual Force (N)	Approximated Force (N)
9.5	5.07	0.04	0.04
9	4.28	0.06	0.07
8.5	3.63	0.08	0.09
8	3.01	0.09	0.11
7.5	2.44	0.11	0.13
7	2.01	0.13	0.15
6.5	1.48	0.15	0.16
6	1.04	0.17	0.18
5.5	0.79	0.19	0.19
5	0.47	0.21	0.20
4.5	0.24	0.23	0.21
4	0.17	0.25	0.21
3.5	0.00	0.26	0.21
3	-0.10	0.28	0.22
2.5	-0.15	0.30	0.22
2	-0.23	0.32	0.22
1.5	-0.27	0.34	0.22
1	-0.29	0.36	0.22

Diode: 33 Transistor: 46 Mass used: 50g

The setup used to carry out this task was explained in the previous section. For the first corner, results using a 100g mass are shown. The results presented for the rest of the corners use a 50g mass. A 100g mass was used only on the first corner because this site seemed to be less sensitive than the other corners.

As you can observe from the tables 3.1-3.4, when the approximated force applied to a site is calculated (according to the methods explained in the

following section), there is a some deviation on most of the readings from what the actual force at that point should be. There could be several explanations for this behavior. But the most likely answer for this phenomenon might be that being on the sensor pad's border means less protective pad covering the inner mechanical parts of the sensor. This can translate into a higher probability of malfunction for the sites along the borders.

Also, as a direct result of this situation, there is less precision of readings on any site which is located on the borders of the sensor. For this reason, the data taken around the corners was not used when trying to interpolate a force from the voltage measures given as an output from the tactile sensor.

3.4 Force Measurement Interpolation

By choosing points at random, measurements were taken throughout the rest of the tactile sensor. All the data sets were plotted to find out the characteristics of the applied force on each one of the selected sites. Several things were discovered in the course of these experiments. The first observation had to do with the maximum voltage at each site. Most of the sites surveyed had a maximum voltage between 10V and 7.5V. There were other sites, not many, where this maximum voltage was much less that 7.5V. This characteristic of the sensor pad indicated a non-uniformity between components inside the pad. It also indicated that the force reading to be

extrapolated from the sensor output voltage is not the same function at each one of the sites.

Table 3.5 Force Interpolation Measurements for Test Point #1

Distance (cm)	Voltage (Volts)	Force (N)	Approx. force (N)
10	9.69	0.01	0.03
9.5	9.63	0.02	0.03
9	9.51	0.03	0.04
8.5	9.4	0.04	0.04
8	9.27	0.05	0.04
7.5	9.08	0.06	0.05
7	8.89	0.07	0.06
6.5	8.67	0.07	0.06
6	8.44	0.08	0.07
5.5	8.19	0.09	0.08
5	7.91	0.10	0.09
4.5	7.56	0.11	0.10
4	7.13	0.12	0.11
3.5	6.8	0.13	0.13
3	6.42	0.14	0.14
2.5	6.06	0.15	0.15
2	5.75	0.16	0.16
1.5	5.41	0.17	0.17
1	5.13	0.18	0.18
0.5	4.87	0.19	0.19

Diode: 10 Transistor: 11 Mass used: 20g

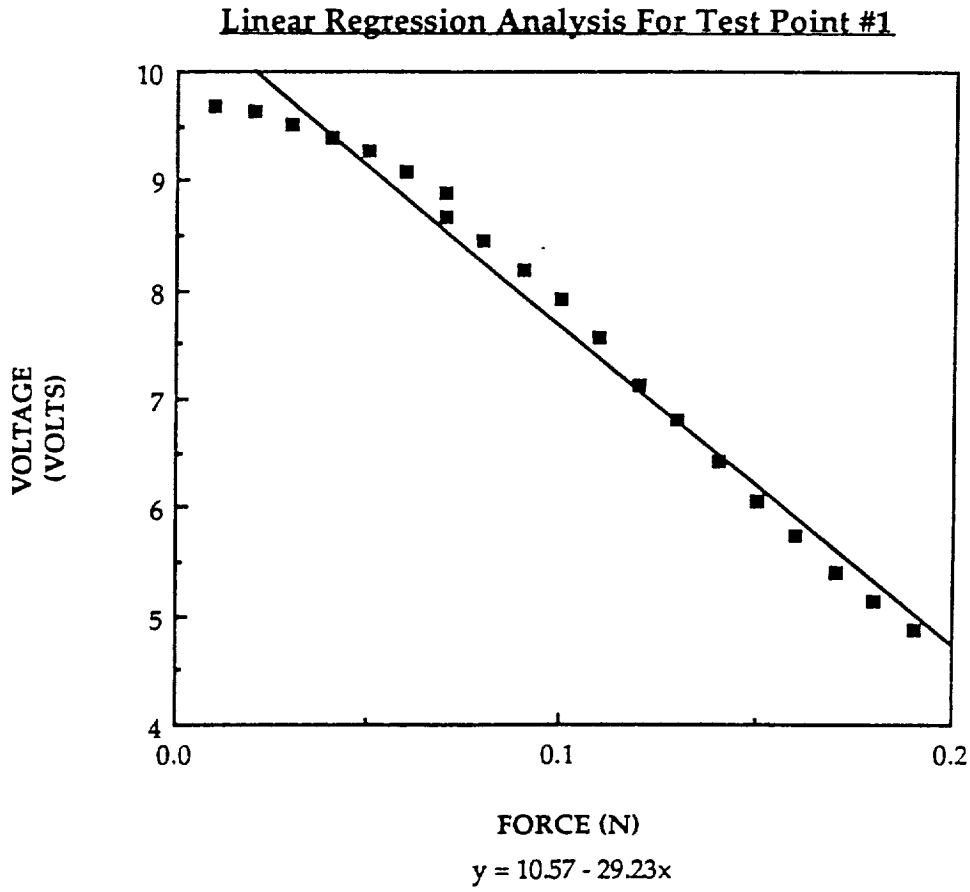

Figure 3.2 Graph Corresponding to the Linear Regression Analysis Done on Test Point #1

Table 3.6 Force Interpolation Measurements for Test Point #2

Distance (cm)	Voltage (Volts)	Force (N)	Approx. force (N)
10	1.43	0.01	0.03
9.5	1.21	0.02	0.04
9	0.93	0.03	0.05
8.5	0.69	0.04	0.06
8	0.46	0.05	0.07
7.5	0.22	0.06	0.07
7	-0.04	0.07	0.08
6.5	-0.37	0.07	0.09
6	-0.57	0.08	0.10
5.5	-0.87	0.09	0.11
5	-1.19	0.10	0.12
4.5	-1.47	0.11	0.13
4	-1.73	0.12	0.14
3.5	-2.02	0.13	0.15
3	-2.31	0.14	0.16
2.5	-2.62	0.15	0.17
2	-2.91	0.16	0.18
1.5	-3.18	0.17	0.19
1	-3.34	0.18	0.19
0.5	-3.72	0.19	0.20

Diode: 26 Transistor: 38 Mass used: 20g

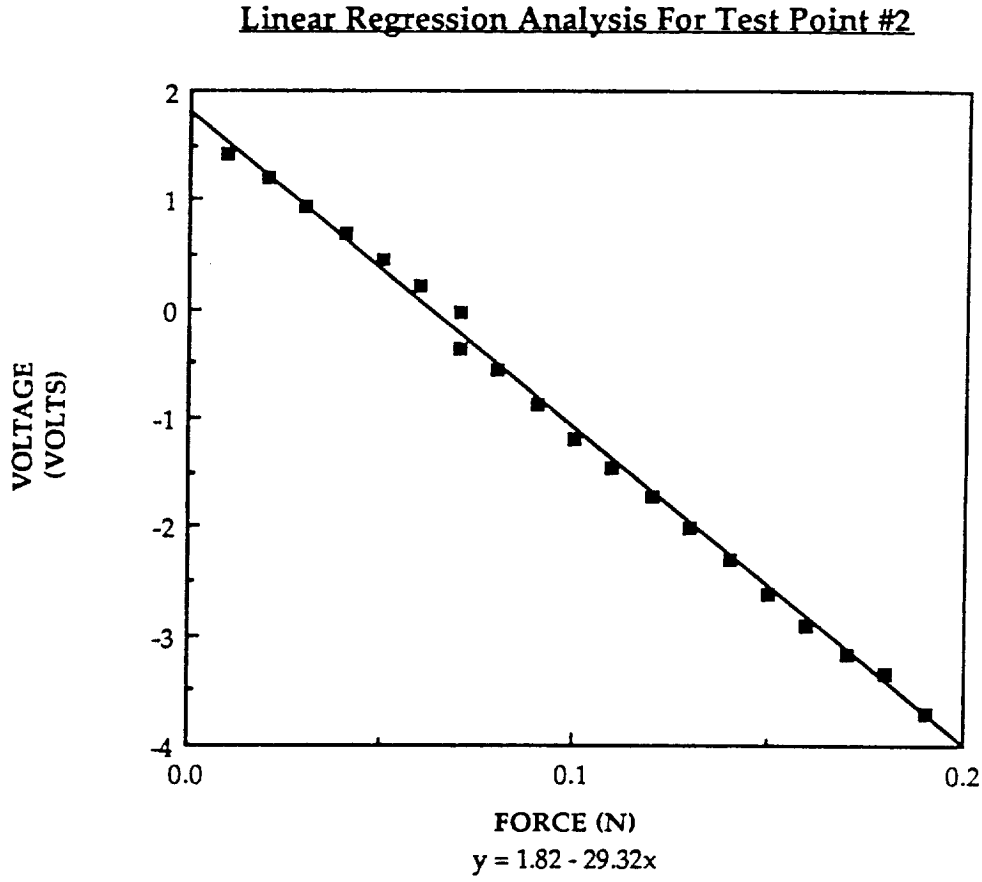

Figure 3.3 Graph Corresponding to the Linear Regression Analysis Done on Test Point #2

Table 3.7 Force Interpolation Measurements for Test Point #3

Distance (cm)	Voltage (Volts)	Force (N)	Approx. force (N)
10	3.75	0.01	0.04
9.5	3.61	0.02	0.04
9	3.45	0.03	0.05
8.5	3.23	0.04	0.06
8	3.07	0.05	0.06
7.5	2.84	0.06	0.07
7	2.61	0.07	0.08
6.5	2.37	0.07	0.08
6	2.1	0.08	0.09
5.5	1.82	0.09	0.10
5	1.56	0.10	0.11
4.5	1.19	0.11	0.12
4	0.71	0.12	0.14
3.5	0.25	0.13	0.16
3	-0.2	0.14	0.17
2.5	-0.67	0.15	0.19
2	-1.15	0.16	0.20
1.5	-1.6	0.17	0.22
1	-2.09	0.18	0.23
0.5	-2.56	0.19	0.25

Diode: 29 Transistor: 41 Mass used: 20g

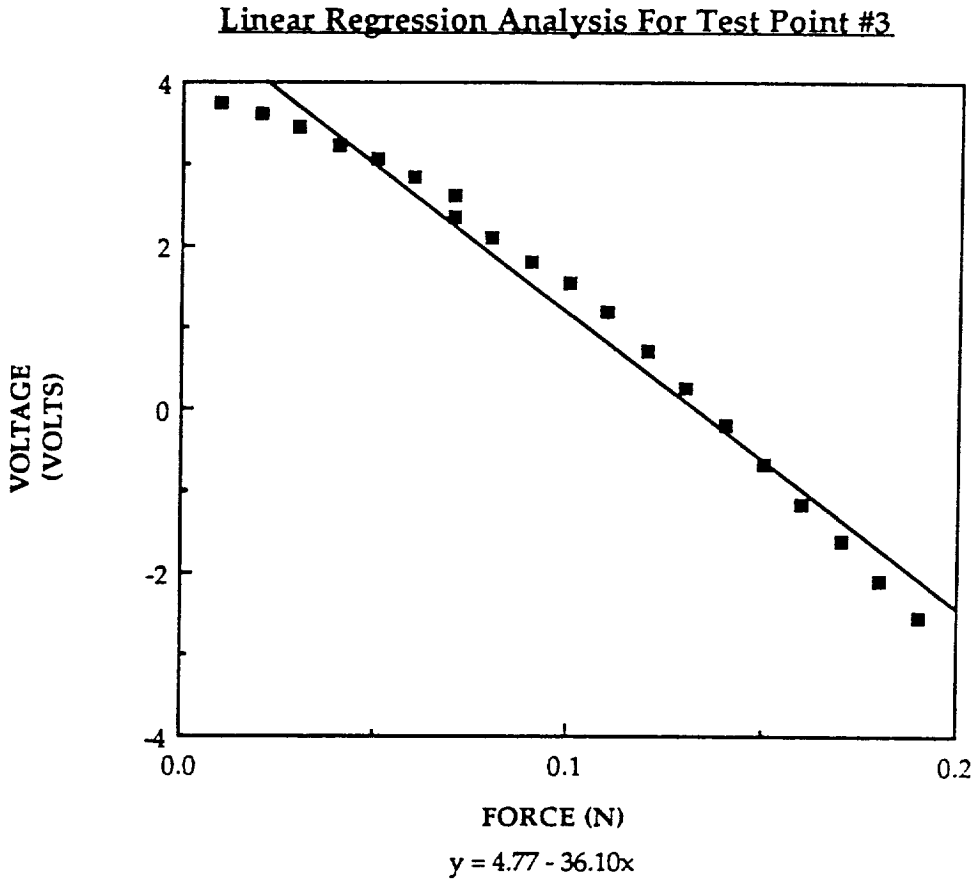

Figure 3.4 Graph Corresponding to the Linear Regression Analysis Done on Test Point #3

Table 3.8 Force Interpolation Measurements for Test Point #4

Distance (cm)	Voltage (Volts)	Force (N)	Approx. force (N)
8.5	10.79	0.04	0.0003
8	10.73	0.05	0.0023
7.5	10.31	0.06	0.02
7	9.94	0.07	0.03
6.5	9.51	0.07	0.04
6	9.19	0.08	0.05
5.5	8.6	0.09	0.07
5	8.05	0.10	0.09
4.5	7.74	0.11	0.10
4	7.04	0.12	0.13
3.5	6.56	0.13	0.14
3	5.97	0.14	0.16
2.5	5.51	0.15	0.18
2	4.92	0.16	0.20
1.5	4.2	0.17	0.22
1	4.04	0.18	0.23
0.5	2.89	0.19	0.26

Diode: 25 Transistor: 38 Mass used: 20g

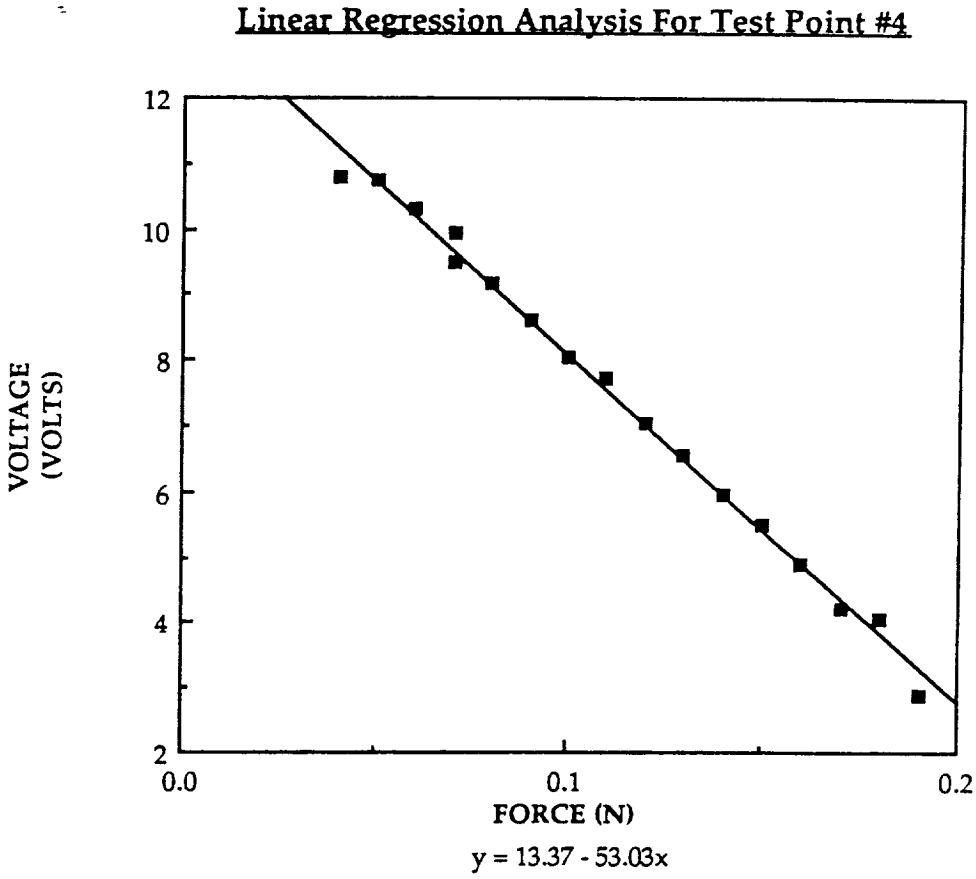

Figure 3.5 Graph Corresponding to the Linear Regression Analysis Done on Test Point #4

The other characteristic of the pad observed was that each one of the sites had a linear region which was consistent throughout most of the data points used. It was also noted that following this linear region, there was a saturation region, where force readings were completely unreliable. After

comparing all the plots for the data sets taken, a linear region that could be applied to each one of the tactile sensor sites was chosen. This region is also considered the safe region for the tactile sensor array. Forces that don't fall within this range could damage the diode-transistor pairs at each of the sites. Before any further analysis took place, I decided that for the rest of the experiments only masses that yield force readings within this linear region should be used. As you can see, this is the case for the test points shown on Figure 3.2, 3.3, 3.4, and 3.5.

After several experiments were done (using only masses that would result in forces within the linear range), a regression analysis was performed. Due to the fact that the voltage when no force is applied in the pad is not uniform throughout the pad, an exponential or higher order regression analysis was not done. In Tables 3.5-3.8 and Figures 3.2-3.5 the results for the linear regression analysis can be observed. Most of the sites on the pad fall within the first or second graphs, having the third and fourth being a special case. From the previously described analysis, an equation which converts a voltage to an applied force was produced. The equation for the applied force has the form:

$$y = mx + b$$

where m is the slope of the equation and b is the y-axis intercept. The b for each one of the sites represents the maximum voltage when no force is applied. The m was carefully chosen using as a guideline the slopes obtained

as a result in the linear regression plots. The final chosen slope for the voltage to force equation was -30.

3.5 Hysteresis Analysis

Hysteresis analysis was also performed to find how reliable the force measurements from the tactile array sensor are. There were three different sets of experiments done on each one of the sites that were studied. Out of all the sites studied, only three will be presented.

The first set of experiments consisted of gradually applying more pressure to a site until reaching the maximum force that could be applied with the chosen mass (see description of the experimental setup). When this maximum force is reach, then gradually unload the sensor until force is no longer applied to the sensor.

From Figures 3.6, 3.7, and 3.8 two observations can be made. The first one is that there exists a discrepancy between the readings taken while loading the sensor (labeled as Voltage 1), and readings taken while unloading the sensor (labeled as Voltage 2). Also noted is that this phenomenon occurs only in some sites. This is the first indication of greater hysteresis effects than were anticipated. As a demonstration that all the sensor sites might not behave the same, the recorded data for test point #1 is shown (Figure 3.6). It seems that this particular sites is extremely sensitive to pressure, therefore creating a narrow range of readings. Before any conclusions were made, another set of tests had to be conducted.

Table 3.9 Hysteresis Data Taken at Test Point #1 for Experiment #1.

Distance (cm)	Force (N)	Voltage 1 (V)	Voltage 2 (V)
10	0.02	-9.89	-9.97
9.5	0.05	-9.98	-10.12
9	0.07	-10.09	-10.26
8.5	0.09	-10.21	-10.38
8	0.12	-10.34	-10.56
7.5	0.14	-10.58	-10.72
7	0.16	-10.67	-10.89
6.5	0.19	-10.85	-10.98
6	0.21	-10.96	-11
5.5	0.23	-11	-11.03
5	0.26	-11.02	-11.03
4.5	0.28	-11.03	-11.04
4	0.30	-11.04	-11.04
3.5	0.33	-11.04	-11.05
3	0.35	-11.05	-11.05
2.5	0.37	-11.05	-11.05
2	0.40	-11.05	-11.06
1.5	0.42	-11.06	-11.06
1	0.44	-11.06	-11.06
0.5	0.47	-11.06	-11.06

Voltage 1: Loading the sensor Voltage 2: Unloading the sensor

Diode: 11 Transistor: 13 Mass used: 50g

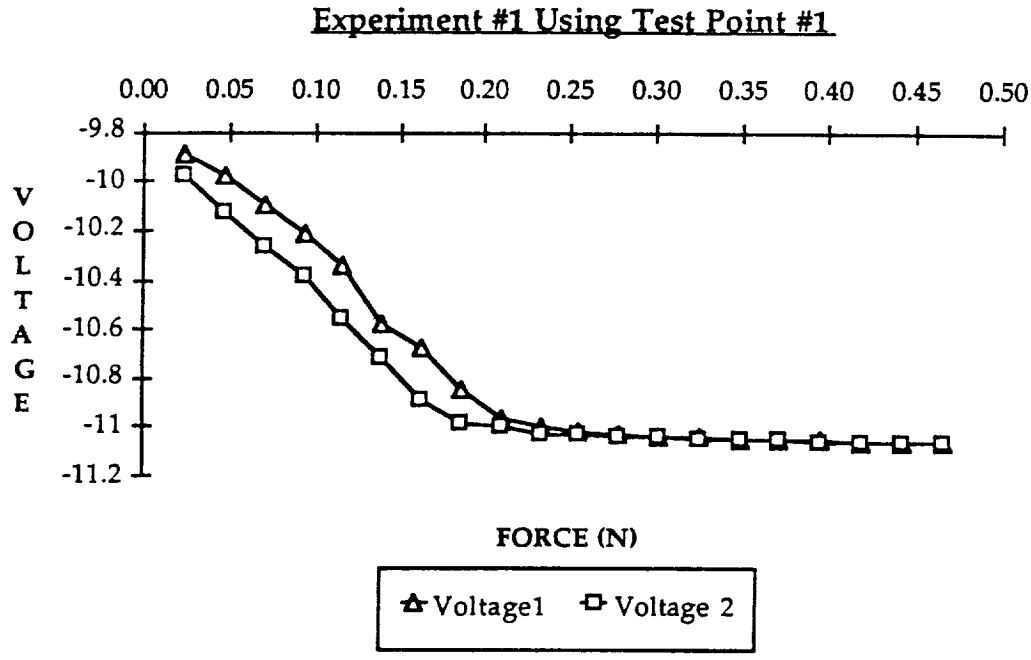

Figure 3.6 Graph Corresponding to Experiment #1 using Test Point #1

Table 3.10 Hysteresis Data Taken at Test Point #2 for Experiment #1

Distance (cm)	Force (N)	Voltage 1 (V)	Voltage 2 (V)
10	0.02	10.8	10.8
9.5	0.05	10.67	8.76
9	0.07	7.44	5
8.5	0.09	4.64	1.8
8	0.12	2.15	-1.01
7.5	0.14	-0.57	-3.27
7	0.16	-2.75	-5.53
6.5	0.19	-4.86	-6.91
6	0.21	-6.31	-8.24
5.5	0.23	-7.84	-9.44
5	0.26	-8.95	-10.6
4.5	0.28	-9.97	-11
4	0.30	-10.98	-11.04
3.5	0.33	-11.04	-11.04
3	0.35	-11.05	-11.05
2.5	0.37	-11.05	-11.06
2	0.40	-11.06	-11.06
1.5	0.42	-11.06	-11.06
1	0.44	-11.07	-11.07

Voltage 1: Loading the sensor Voltage 2: Unloading the sensor

Diode: 22 Transistor: 25 Mass used: 50g

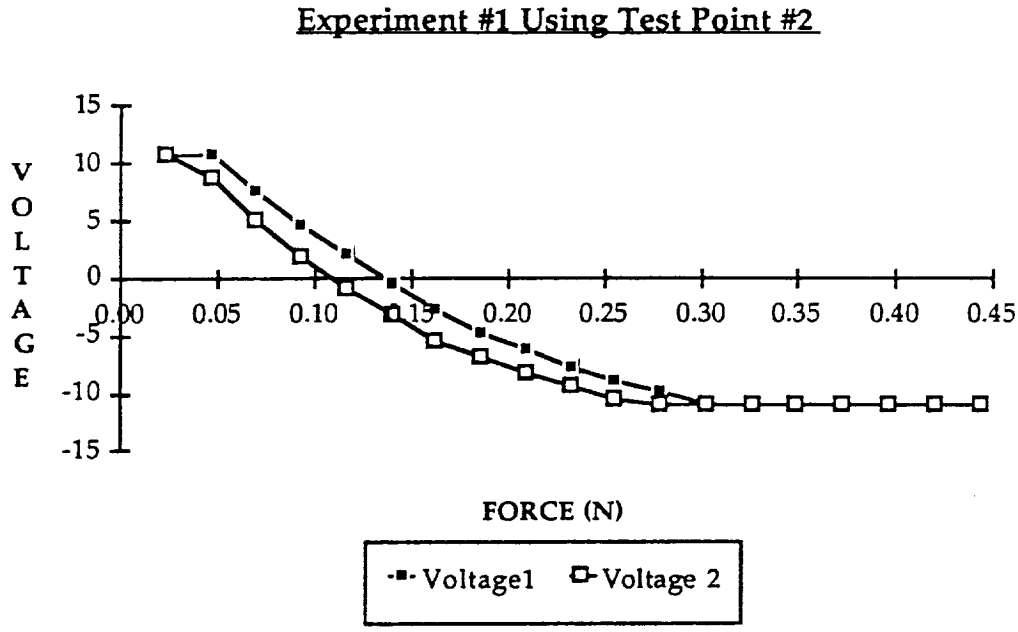

Figure 3.7 Graph Corresponding to Experiment #1 using Test Point #2

Table 3.11 Hysteresis Data Taken at Test Point #3 for Experiment #1.

Distance (cm)	Force (N)	Voltage 1 (V)	Voltage 2 (V)
10	0.02	10.83	10.83
9.5	0.05	9.84	8.59
9	0.07	7.52	6
8.5	0.09	5.15	3.91
8	0.12	3.16	2
7.5	0.14	1.52	0.13
7	0.16	-0.25	-1.81
6.5	0.19	-2.19	-3.75
6	0.21	-3.84	-5.46
5.5	0.23	-5.54	-7.01
5	0.26	-6.84	-8.33
4.5	0.28	-8.51	-9.49
4	0.30	-9.83	-10.33
3.5	0.33	-10.19	-11
3	0.35	-11	-11.03
2.5	0.37	-11.04	-11.05
2	0.40	-11.05	-11.05
1.5	0.42	-11.05	-11.05
1	0.44	-11.05	-11.06
0.5	0.47	-11.06	-11.06

Voltage 1: Loading the sensor Voltage 2: Unloading the sensor

Diode: 28 Transistor: 32 Mass used: 50g

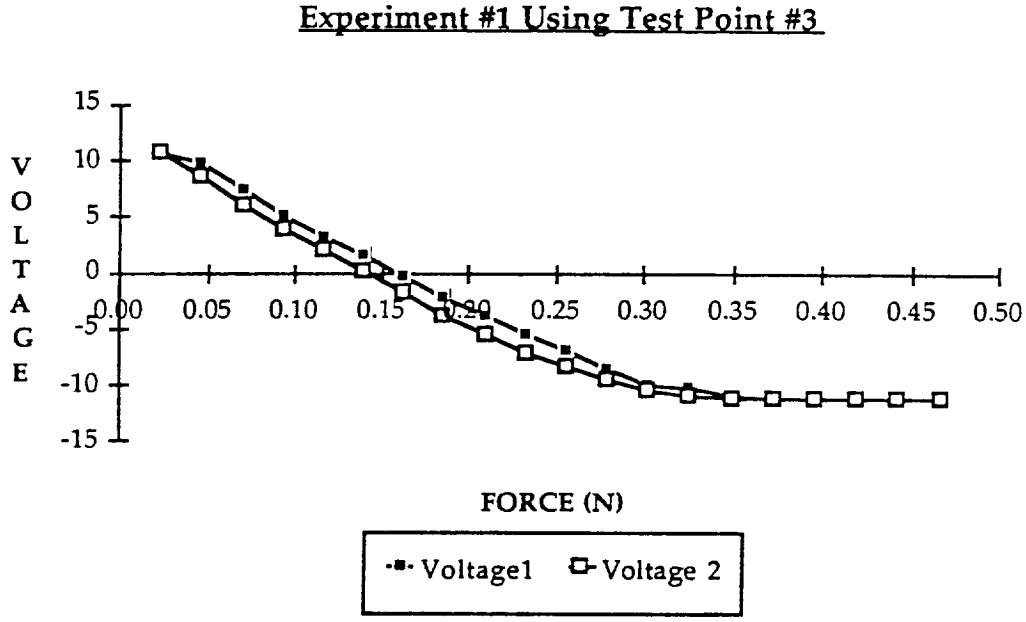

Figure 3.8 Graph Corresponding to Experiment #1 using Test Point #3

The second set of experiments consisted of taking measurements by first loading the sensor applying a force. Then, before applying further pressure to get the next voltage reading, I completely unloaded the sensor until it reached the original reading when no force was applied.

Table 3.12 Hysteresis Data Taken at Test Point #1 for Experiment #2.

Distance (cm)	Force (N)	Voltage 1 (V)	Voltage 2 (V)
10	0.02	-9.94	-9.95
9.5	0.05	-9.98	-10
9	0.07	-10.04	-10.04
8.5	0.09	-10.11	-10.12
8	0.12	-10.2	-10.21
7.5	0.14	-10.25	-10.28
7	0.16	-10.36	-10.37
6.5	0.19	-10.43	-10.46
6	0.21	-10.55	-10.55
5.5	0.23	-10.64	-10.67
5	0.26	-10.71	-10.75
4.5	0.28	-10.85	-10.87
4	0.30	-10.95	-10.96
3.5	0.33	-10.98	-10.99
3	0.35	-10.99	-11
2.5	0.37	-11	-11.03
2	0.40	-11.03	-11.03
1.5	0.42	-11.03	-11.03
1	0.44	-11.04	-11.04
0.5	0.47	-11.04	-11.05

Diode: 11 Transistor: 13 Mass used: 50g

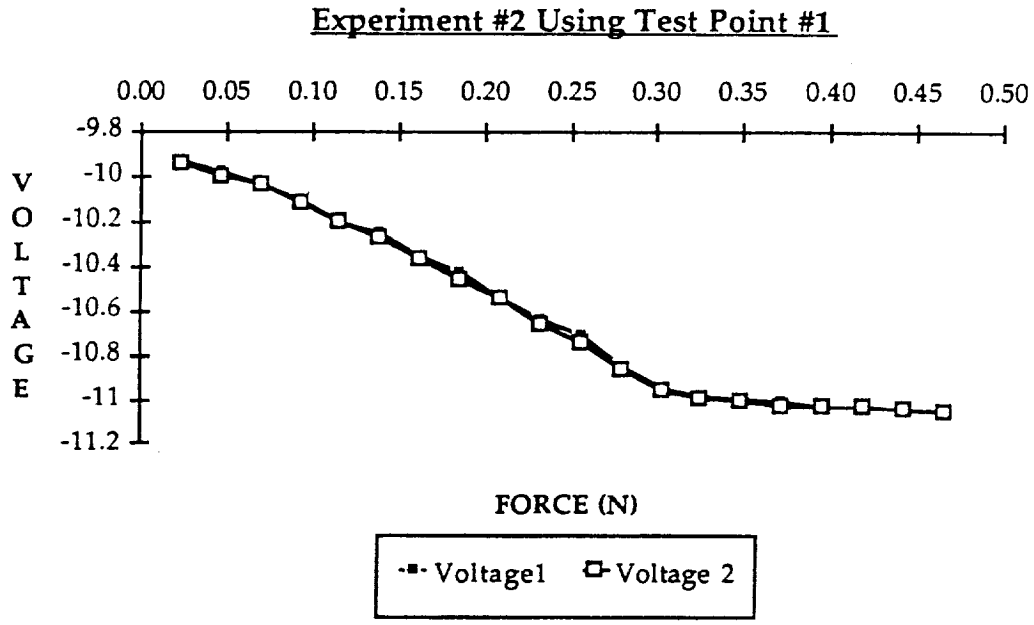

Figure 3.9 Graph for Experiment #2 using Test Point #1

Table 3.13 Hysteresis Data Taken at Test Point #2 for Experiment #2.

Distance (cm)	Force (N)	Voltage 1 (V)	Voltage 2 (V)
10	0.02	10.82	10.6
9.5	0.05	10.08	7.52
9	0.07	6.47	4.3
8.5	0.09	3.66	1.86
8	0.12	1.13	-0.56
7.5	0.14	-1.23	-2.82
7	0.16	-3.59	-4.77
6.5	0.19	-5.41	-6.31
6	0.21	-6.91	-7.58
5.5	0.23	-8.11	-8.74
5	0.26	-9.15	-9.78
4.5	0.28	-10.19	-10.82
4	0.30	-10.92	-11.03
3.5	0.33	-11.03	-11.04
3	0.35	-11.04	-11.05
2.5	0.37	-11.05	-11.06
2	0.40	-11.06	-11.06
1.5	0.42	-11.06	-11.07
1	0.44	-11.06	-11.07

Diode: 22 Transistor: 25 Mass used: 50g

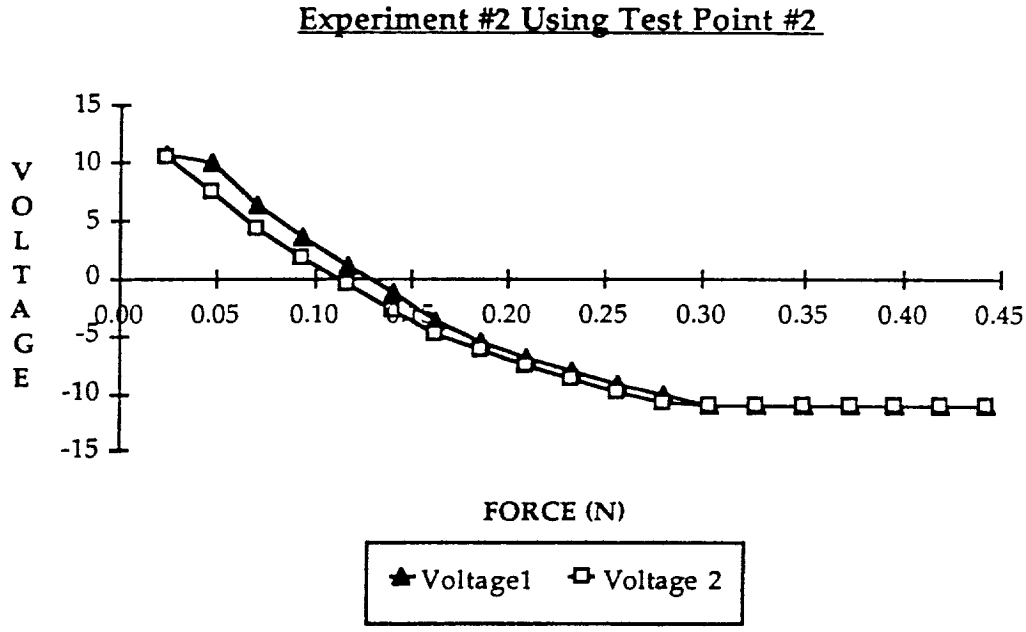

Figure 3.10 Graph for Experiment #2 using Test Point #2

Table 3.14 Hysteresis Data Taken at Test Point #3 for Experiment #2.

Distance (cm)	Force (N)	Voltage 1 (V)	Voltage 2 (V)
10	0.02	10.82	10.78
9.5	0.05	10.66	9.77
9	0.07	9.25	8.45
8.5	0.09	7.91	7.28
8	0.12	6.61	5.99
7.5	0.14	5.33	4.93
7	0.16	4.12	3.78
6.5	0.19	2.76	2.61
6	0.21	1.81	1.63
5.5	0.23	0.61	0.6
5	0.26	-0.24	-0.41
4.5	0.28	-1.32	-1.37
4	0.30	-2.36	-2.52
3.5	0.33	-3.31	-3.52
3	0.35	-4.25	-4.59
2.5	0.37	-5.32	-5.3
2	0.40	-6.03	-6.23
1.5	0.42	-7.09	-7.21
1	0.44	-7.73	-7.86
0.5	0.47	-8.11	-8.46

Diode: 28 Transistor: 32 Mass used: 50g

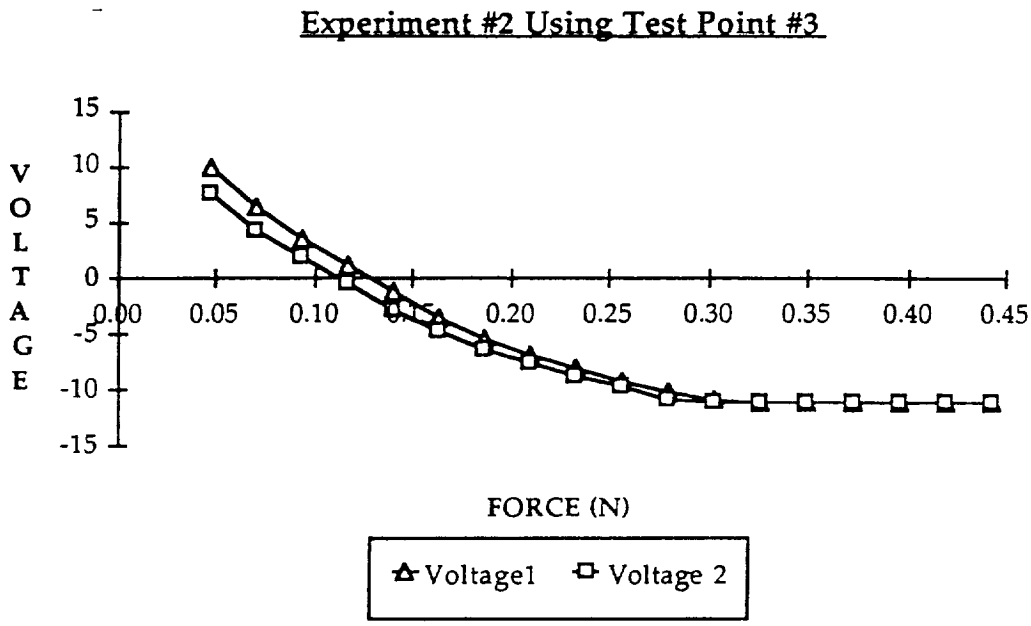

Figure 3.11 Graph for Experiment #2 using Test Point #3

Figures 3.9-3.11 belong to this set of experiments. In these figures, Voltage 1 refers to the voltage reading taken using the method explained above, and Voltage 2 refers to the readings taken by slowly applying more force without first unloading the sensor. Again, the same problems observed in the previous test are present on this one. These problems are the discrepancy between readings for the same force, and also the fact that this is not true for all the points.

Finally, a third set of experiments was done. Measurements for these tests were taken by first choosing an initial applied force to the sensor and then loading and unloading the sensor about that force. Here an important observation was made: when the range of loadings/unloadings about a force

is large (more than ± 0.08 N of the chosen force), the sensor readings fluctuate enough to be unreliable. However, if the range is smaller, then the force readings stay within a 5% of what they are supposed to be.

Table 3.15 Hysteresis Data Taken at Test Point #1 for Experiment #3.

		RUNS OF THE EXPERIMENT									
distance (cm)	Force (N)	1	2	3	4	5	6	7	8	9	10
10	0.01									-9.95	-9.97
9.5	0.02								-9.97	-9.97	-9.98
9	0.03							-9.99	-9.98	-9.99	-9.99
8.5	0.04						-9.99	-10.01	-10	-10.01	-10.02
8	0.05					-10.01	-10.01	-10.02	-10.02	-10.02	-10.03
7.5	0.06				-10.03	-10.03	-10.03	-10.04	-10.04	-10.04	-10.04
7	0.07			-10.07	-10.06	-10.06	-10.06	-10.07	-10.08	-10.08	-10.08
6.5	0.07		-10.07	-10.09	-10.08	-10.09	-10.09	-10.09	-10.1	-10.1	-10.09
6	0.08	-10.11	-10.1	-10.11	-10.1	-10.11	-10.11	-10.11	-10.12	-10.11	-10.11
5.5	0.09	-10.14	-10.12	-10.11	-10.12	-10.12	-10.12	-10.12	-10.13	-10.13	-10.13
5	0.10	-10.16	-10.13	-10.15	-10.14	-10.14	-10.14	-10.14	-10.15	-10.16	-10.16
4.5	0.11		-10.18	-10.19	-10.18	-10.18	-10.16	-10.19	-10.19	-10.21	-10.2
4	0.12			-10.21	-10.21	-10.21	-10.22	-10.22	-10.22	-10.23	-10.23
3.5	0.13				-10.23	-10.24	-10.25	-10.25	-10.25	-10.26	-10.26
3	0.14					-10.27	-10.28	-10.27	-10.28	-10.28	-10.29
2.5	0.15						-10.32	-10.32	-10.32	-10.33	-10.32
2	0.16							-10.34	-10.35	-10.35	-10.35
1.5	0.17								-10.38	-10.38	-10.38
1	0.18									-10.44	-10.42

Diode: 11 Transistor: 13 Mass used: 20g

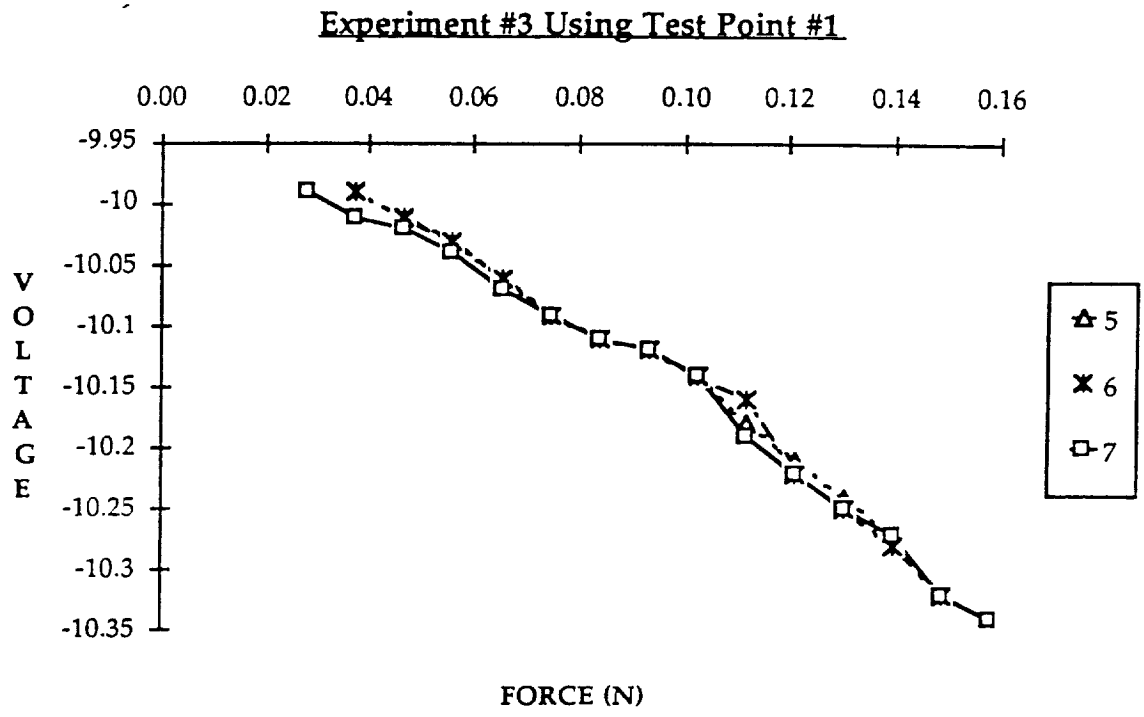

Figure 3.12 Data Gathered for Experiment #3 using Test Point #1. Runs 5, 6, and 7 of the Experiment were Plotted

Table 3.16 Hysteresis Data Taken at Test Point #2 for Experiment #3.

		RUNS OF THE EXPERIMENT									
distance (cm)	Force (N)	1	2	3	4	5	6	7	8	9	10
7	0.07			4.63	4.44						
6.5	0.07		3.46	3.37	3.5	3.54	3.49	3.59	3.43	3.56	3.46
6	0.08	2.68	2.52	2.71	2.41	2.61	2.51	2.42	2.47	2.63	2.39
5.5	0.09	2.01	1.61	1.62	1.71	1.81	1.72	1.66	1.56	1.68	1.62
5	0.10	0.84	0.71	0.55	0.66	0.7	0.83	0.63	0.54	0.58	0.58
4.5	0.11		0.24	-0.27	-0.4	-0.2	-0.23	-0.27	-0.24	-0.36	-0.33
4	0.12			-1.13	-1.21						

Diode: 22 Transistor: 25 Mass used: 20g

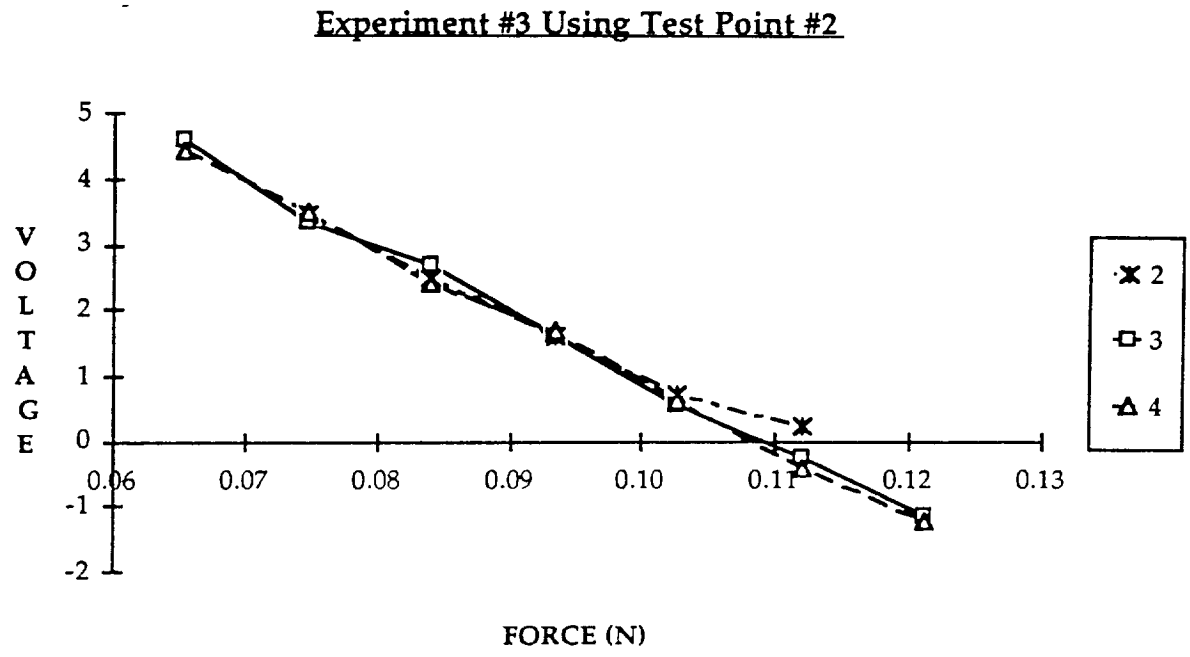

Figure 3.13 Data gathered for Experiment #3 using Test Point #2. Runs 2, 3, and 4 of the Experiment were Plotted

Table 3.17 Hysteresis Data Taken at Test Point #3 for Experiment #3.

		RUNS OF THE EXPERIMENT									
distance (cm)	Force (N)	1	2	3	4	5	6	7	8	9	10
6.5	0.07		4.03	4	3.97	3.97	4.01	3.94	3.88	3.98	3.97
6	0.08	3.25	3.07	2.96	3.12	3.04	3.04	3.12	3.11	3.01	2.89
5.5	0.09	2.61	2.23	2.23	2.64	2.1	2.33	2.14	2.29	2.32	2.7
5	0.10	1.51	1.54	1.62	1.41	1.48	1.78	1.48	1.32	1	1.63
4.5	0.11		0.95	0.49	0.69	0.52	0.63	0.54	0.55	0.46	0.43

Diode: 28 Transistor: 32 Mass used: 20g

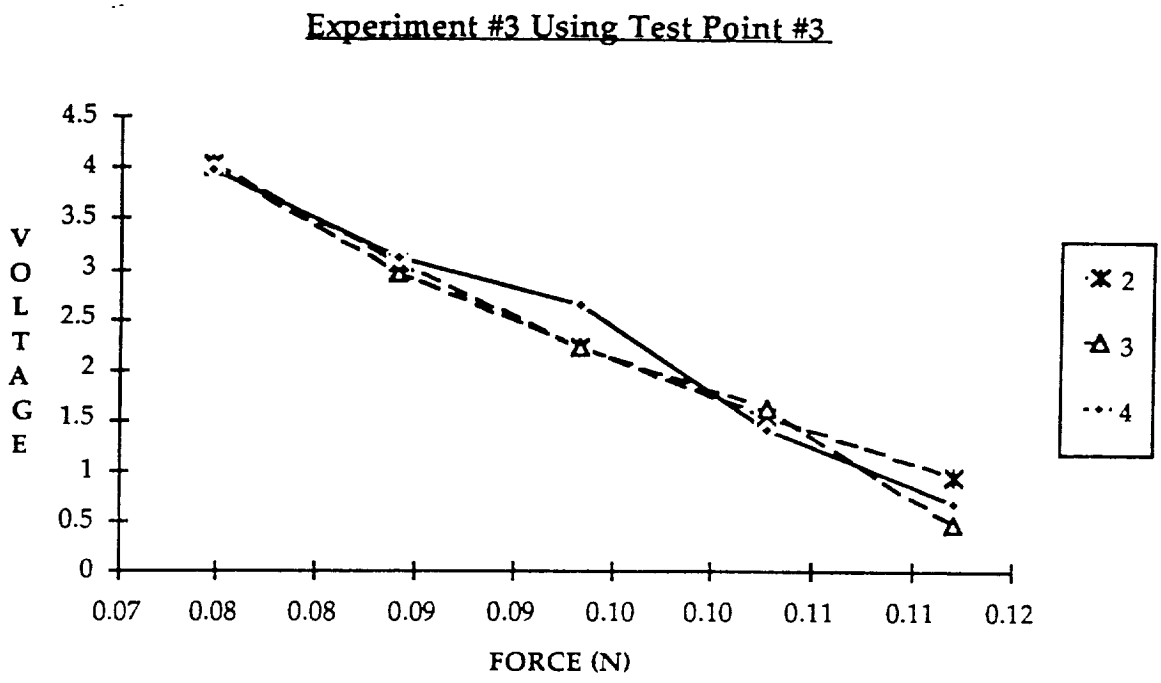

Figure 3.14 Data Gathered for Experiment #3 using Test Point #3. Runs 2, 3, and 4 of the Experiment were Plotted.

3.6 Sensitivity Analysis

The next set of experiments were aimed to discover how sensitive the tactile sensor pad is. In order to perform these experiments, the control and communication software written for the tactile sensor was used.

Two objects, at different times, were pressed against the surface of the sensor pad: a circular object and a rectangular object. Before each one of these tests took place, a reading of the unloaded sensor pad was taken. Then, an

object was applied to the pad surface, and immediately another scan of the sensor was done. In order to check whether the pressed object was actually sensed by the pad, the data for the unloaded sensor was subtracted from the data for the loaded sensor.

The results of these experiments are shown on Figure 3.15 to Figure 3.20, and for each one of the objects applied, a contour and a mesh graph of the sensor pad were drawn. In Figure 3.16, a rectangular object pressed diagonally on the sensor pad surface can be seen. In the previous figure (Fig. 3.15), a contour graph of the same experiment is plotted. In this graph you can notice that where the object is not applied, sometimes there are some small voltage drop readings. This is due to some error introduced to the system by the A/D converter. Nevertheless, this voltage drop reading has a magnitude of 0.094 V (in its worst case), introducing only a 1.56% of error to the sensor sensitivity. You can notice this same phenomenon in each one of the contour graphs drawn for the rest of the experiments.

The other two experiments performed on the sensor pad consisted on applying a circular object to the pad surface. In one case the circular object was applied to the left, and in the other case it was applied to the right. As it can be seen from the mesh graphs (Figure 3.18 and 3.20), the sensor pad is deformed according to the shape of the applied force.

On and off during the course of these experiments some change in force (Δ) appears on the diode-transistor pairs (1,1) and (17,19), even though no force was applied at this moment. It seems that on a previous project where this tactile sensor was also used, the behavior of the first diode-transistor pair (1,1) was noticed but not of the second diode-transistor pair.

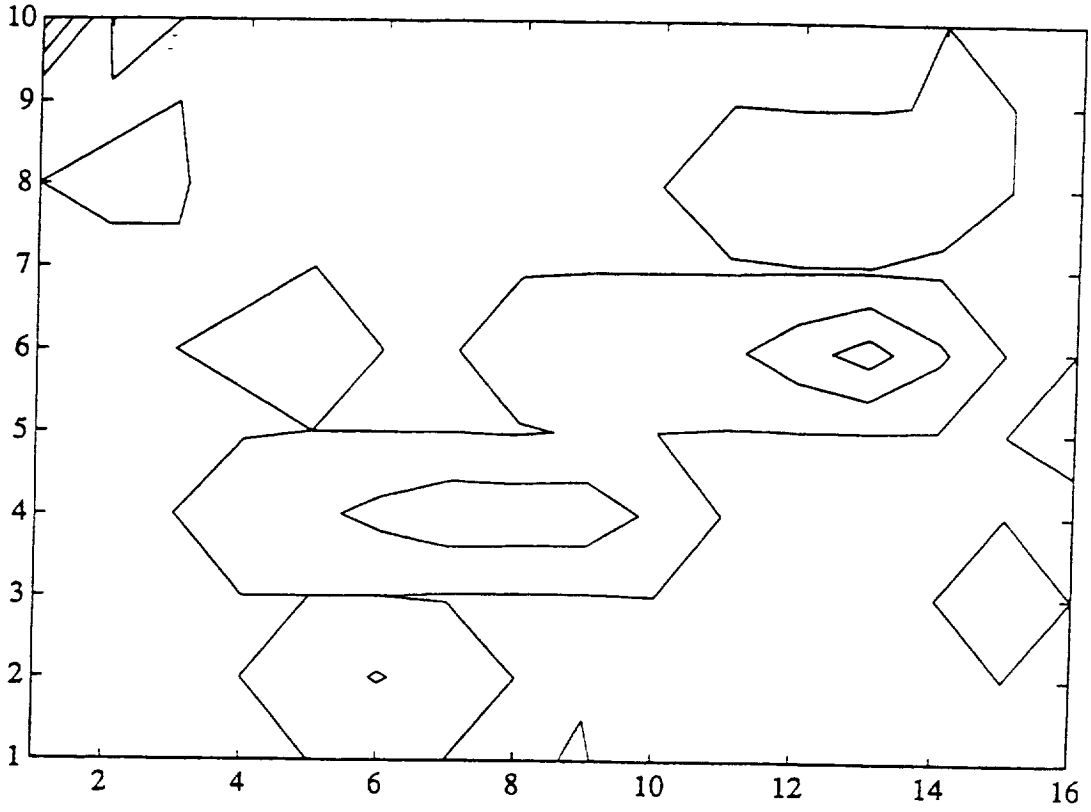

Figure 3.15 Contour Plot of the Sensor Pad Showing an Applied Diagonal Force.

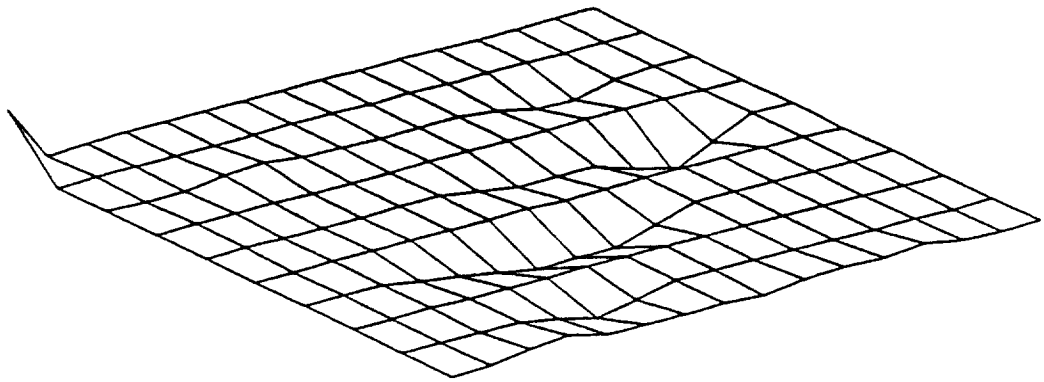

Figure 3.16 Mesh Plot of the Sensor Pad Showing an Applied Diagonal Force.

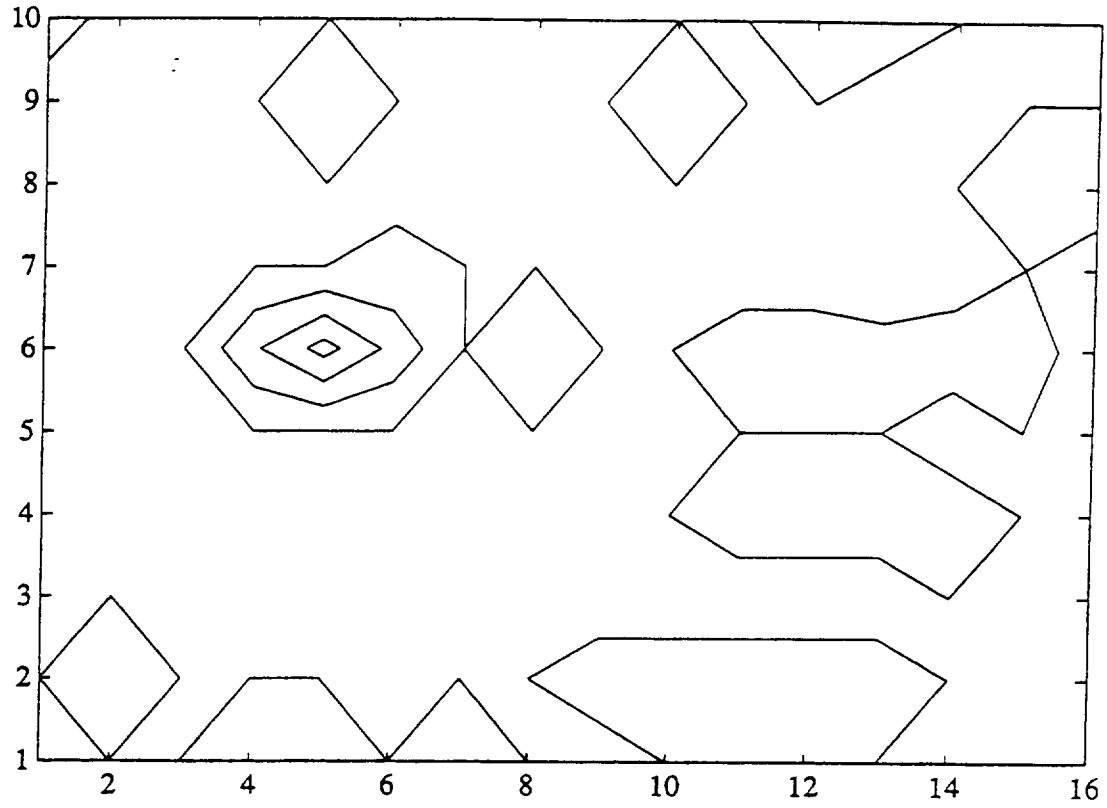

Figure 3.17 Contour Plot of the Sensor Pad Showing a Circular Object Pressed Against the Left Side of the Pad.

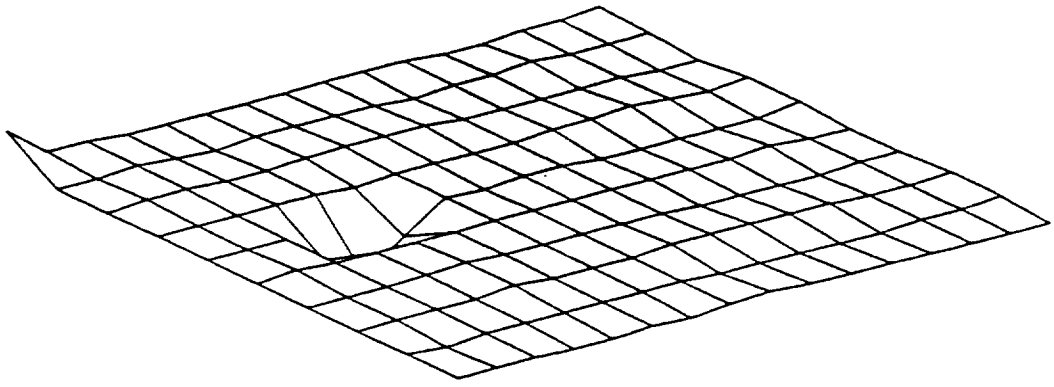

Figure 3.18 Mesh Plot of the Sensor Pad Showing a Circular Object Pressed Against the Left Side of the Pad.

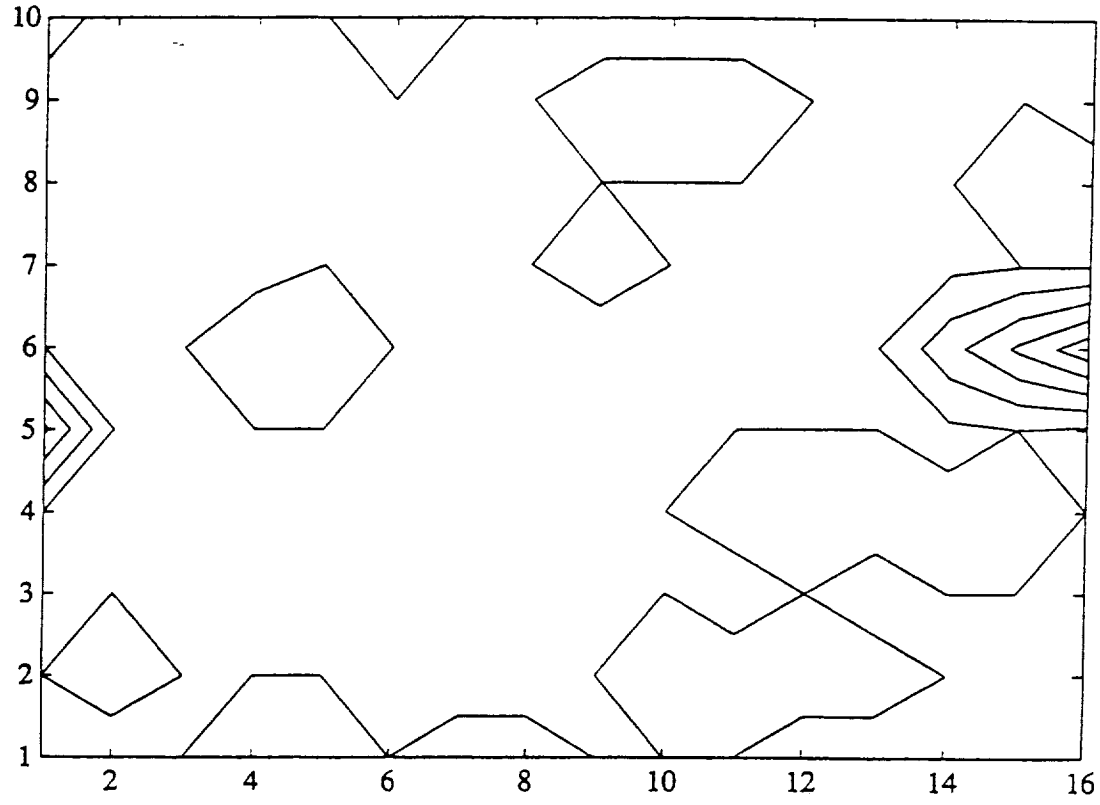

Figure 3.19 Contour Plot of the Sensor Pad Showing a Circular Object Pressed Against the Right Side of the Pad.

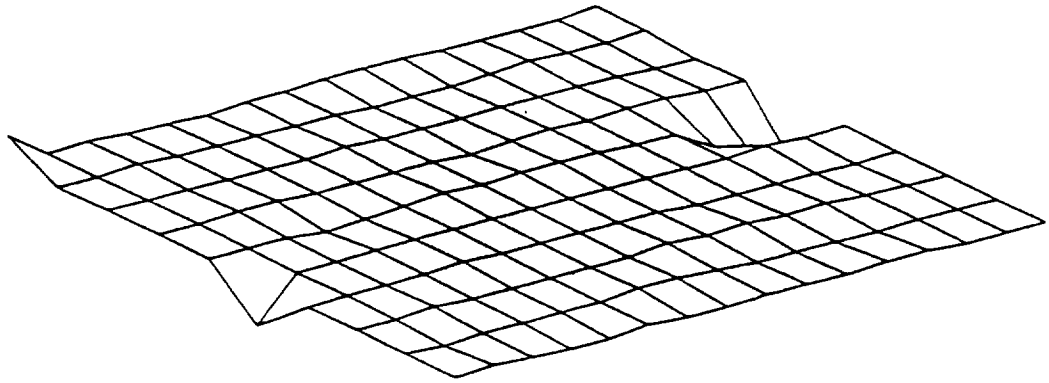

Figure 3.20 Mesh Plot of the Sensor Pad After a Circular Object Pressed Against the Right Side of the Pad.

(17,19) [4]. The Δ for the first diode transistor pair every time it occurs is the same; its magnitude is 4.63 V. The same behavior occurs in the other diode-transistor pair mentioned, but in this one the magnitude of the Δ is 1.70V. This phenomenon is probably due to some malfunction of these diode-transistor pairs inside the pad at this location.

3.7 Effects of an Applied Force on its Neighbors

Another aspect of the tactile sensor that was studied dealt with how an applied force to a site affected its nearest neighbors. It was observed that as long the applied force to a site was less than 0.857 Newtons, there was no force reading recorded on the nearest neighbors. If the applied force to a point was greater than this, then force readings would be sensed at the nearest neighbors and probably some type of damage to the selected diode-transistor pair could result.

CHAPTER 4

SENSOR INTERFACE WITH THE 68HC11 EVALUATION BOARD

A 68HC11 EVB was chosen as the controlling microprocessor for this sensor system. The reasons behind this decision are the low cost and ease of use of this microprocessor.

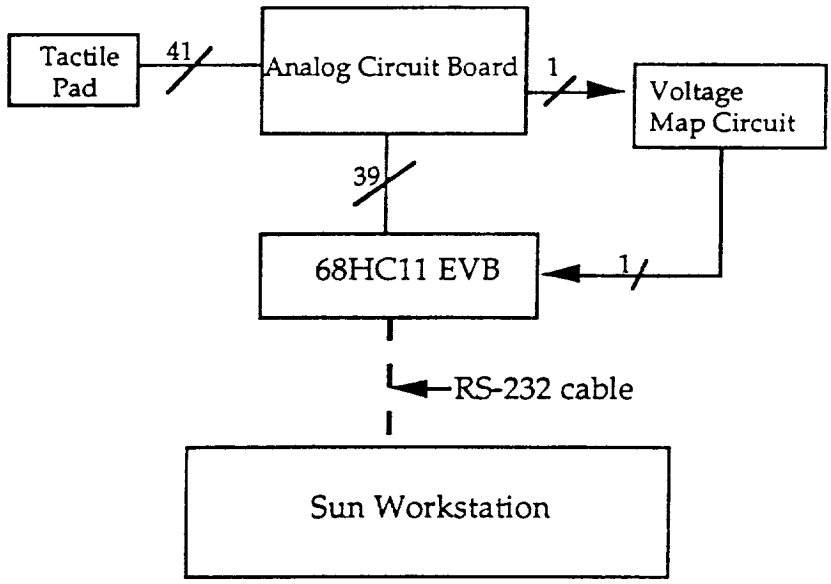

Figure 4.1 Hardware Configuration for the Tactile Sensing System

4.1 Hardware Configuration

The final hardware interface, as seen in Fig 4.1, consists of the tactile sensor pad connected to the analog board of the old sensor. The cable used for this connection is the same one that was used in the old sensor.

Table 4.1 Connections between Analog Board and 68HC11 EVB

Analog Board Jumper	Description	68HC11 EVB Connections	Description
1	5V	26	Vdd
2	5V	26	Vdd
3	GND	1	GND
4	GND	1	GND
5	Pin 6-U18	1	GND
6	Pin 3-VR2	1	GND
7	Analog GND	1	GND
8	Pin 3-S1, Pin 7-U17	Not Connected	Not Connected
9	Pin 1-U16, Pin 2-U16	Not Used	Not Used
10	Pin 10-U17	26	Vdd
11	Pin 9-U17	1	GND
12	Pin 8-U17	26	Vdd
13	Pin1 and 2-S2	26	Vdd
14	Not Connected	Not Connected	Not Connected
15	Not Connected	Not Connected	Not Connected
16	Not Connected	Not Connected	Not Connected
17	Not Connected	Not Connected	Not Connected
18	Pin 11-U18	12	PC3
19	Pin 10-U18	13	PC4
20	Pin 9-U18	14	PC5
21	Pin 11-U19	9	PC0
22	Pin 10-U19	10	PC1
23	Pin 9-U19	11	PC2
24	Not Connected	Not Connected	Not Connected
25	Pin 8-S1	1	GND
26	Not Connected	Not Connected	Not Connected
27	Not Connected	Not Connected	Not Connected
28	Pin 10-U15	39	PB3
29	Pin 11-U15	38	PB4
30	Pin 14-U15	37	PB5
31	Pin 13-U15	36	PB6
32	Pin 11-U14	42	PB0
33	Pin 10-U14	41	PB1
34	Pin 9-U14	40	PB2
35	-12V	Not Used	Not Used
36	-12V	Not Used	Not Used
37	Analog GND	1	GND
38	Analog GND	1	GND
39	+12V	Not Used	Not Used
40	+12V	Not Used	Not Used

The analog board is connected to the 68HC11 by means of their respective jumpers. In Table 4.1 the connections between the analog board and the 68HC11 EVB are detailed. Finally, the 68HC11 EVB is connected to a Sun workstation by a RS-232 cable.

Table 4.2 List of Diodes on the Sensor Pad and Configuration for Port C so they can be Activated.

DIODE	PORT C CONFIG.
1	'$04'
2	'$0D'
3	'$14'
4	'$1C'
5	'$24'
6	'$2C'
7	'$34'
8	'$3C'
9	'$03'
10	'$0B'
11	'$13'
12	'$1B'
13	'$23'
14	'$2B'
15	'$33'
16	'$3B'
17	'$04'
18	'$0A'
19	'$12'
20	'$1A'

DIODE	PORT C CONFIG.
21	'$22'
22	'$2A'
23	'$32'
24	'$3A'
25	'$01'
26	'$09'
27	'$11'
28	'$19'
29	'$21'
30	'$29'
31	'$31'
32	'$39'
33	'$00'
34	'$08'
35	'$10'
36	'$18'
37	'$20'
38	'$28'
39	'$30'
40	'$38'

Table 4.3 List of Transistors on the Sensor Pad and Configuration for Port B so they can be Activated.

TRANSISTOR	PORT B CONFIG.
1	'$05'
2	'$0D'
3	'$15'
4	'$1D'
5	'$25'
6	'$2D'
7	'$35'
8	'$3D'
9	'$45'
10	'$04'
11	'$0C'
12	'$14'
13	'$1C'
14	'$24'
15	'$2C'
16	'$34'
17	'$3D'
18	'$44'
19	'$03'
20	'$0B'
21	'$13'
22	'$1B'
23	'$23'
24	'$2B'
25	'$33'
26	'$3B'
27	'$43'

TRANSISTOR	PORT B CONFIG.
28	'$02'
29	'$0A'
30	'$12'
31	'$1A'
32	'$22'
33	'$2A'
34	'$32'
35	'$3A'
36	'$42'
37	'$01'
38	'$09'
39	'$11'
40	'$19'
41	'$21'
42	'$29'
43	'$31'
44	'$39'
45	'$45'
46	'$06'
47	'$08'
48	'$10'
49	'$18'
50	'$20'
51	'$28'
52	'$30'
53	'$38'
54	'$40'

4.2 68HC11 EVB Port Assignment

Out of the 4 existing parallel I/O ports in the 68HC11 EVB, only three are used. These ports are B, C, and E. Port C selects the desired diode, and port B the transistor. Each port controls two multiplexers on the analog board, one corresponding to the column and the other to the row where the desired component is located. The last port used, port E, is the input port for the built-in A/D converter.

4.2.1 Port B of the 68HC11 EVB

As it was mentioned before, Port B selects which transistor is going to be activated. The higher 4 bits (PB3-PB6) are used to select the row, and the lower 3 bits (PB0-PB2) select the column. Table 4.2 shows a list of all the transistors in the tactile pad, and how Port B should be configured in order to activate a specific transistor.

4.2.2 Port C of the 68HC11 EVB

Port C selects which diode is going to be activated. The higher 3 bits (PC3-PC5) are used to select the row, and the lower 3 bits (PC0-PC2) select the column. Table 4.3 shows a list of all the diodes on the pad and how Port C should be configured so a desired diode can be activated.

4.2.2 Port E of the 68HC11 EVB

Port E of the 68HC11 EVB has a dual role. Its serves as an I/O parallel port and also as the input for the built-in A/D converter. There are 8 input lines to port E but only one channel was needed. The assigned bit was bit PE1. Bit PE0 of this port could not be used as the input to the A/D because upon reset, the monitor program in the 68HC11 checks the state of PE0. If a low state is detected, the monitor program is executed and the prompt displayed. If a high state is detected, the monitor will automatically jump to the EEPROM and execute the users code. If the output of the voltage map circuit is connected to PE0, upon reset it might confuse the monitor program and the program might jump to an unknown location.

CHAPTER 5

SOFTWARE DESCRIPTION AND SYSTEM OPERATION

5.1 Initialization

5.1.1 Power Up Initialization

Upon power up, the 68HC11 EVB starts executing the instructions starting at $E000. Two registers, the OPTION and the TMSK2, have to be initialize within 64 bus-cycles after power-up. If this period of time expires before these registers are configured, some of the bits in these registers become read-only and they can not be change.

5.1.2 SCI Initialization

The SCI is the serial port used for communication with the host computer. At this time, this serial port is configured to 1 start bit, 8 data bits, and 1 stop bit. Also the baud rate, 9600, and the clock speed, 8 Mhz EXTAL are set. Note that there is another port, the terminal I/O port, which uses the ACIA and is not used in this project.

5.1.3 A/D Converter Initialization

When the OPTION register is initialize at power up, two of its bits (ADPU and CSEL), have to be set properly. If this bits are not

correctly initialized, the A/D converter will not be operational. The A/D converter is by default not activated, therefore the ADPU bit has to be set in order to enable it.

The CSEL bit has to be set to zero in order to minimize the conversion errors if the alternate clock source is selected during the A/D conversion.

5.2 Software Location on Memory

The communication and data acquisition programs are located starting at address $E000 on the 68HC11 EVB Monitor EEPROM. This assembler code is designed to replace the Buffalo monitor located originally at this location.

5.3 Communication Software between Host and 68HC11 EVB

Before any code was written, a communication protocol between the 68HC11 EVB and the host computer (Sun workstation) had to be defined. Having only two functions to implement, simplifies the final design. Each time one of the functions is invoked, the host communicates the desired operation to the EVB and it initiates execution. Before the EVB begins execution, an acknowledgment of the requested command is sent to the host. This is implemented as a safety feature. When the end of the desired information is reached, a delimiter indicating end of transmission is sent.

5.3.1 Host Communication Software

The host in this system is a Sun workstation which is connected to a 68HC11 EVB using the serial port. This port is labeled as Host I/O in the EVB Manual, and the cable used for communication is a regular modem cable [5]. The software developed for the host consists mainly of two parts: transmitting or receiving data using Port B of the workstation, and changing the received ASCII characters into a 16-bit integer format. Instead of sending integers through the communication line, ASCII characters are used because that is the only type the host can read or write.

Before transmitting or receiving any data, the port had to be initialized and configured. A pointer to the I/O port had to be set up before any communication took place, and the data word characteristics had to be

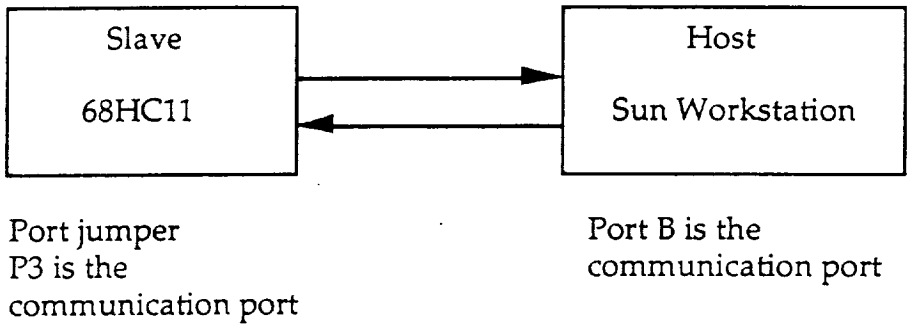

Figure 5.1 Host - Slave Software Configuration

determined. Usually the Sun workstations are configured as 1 start bit, 7 data bits, and 1 stop bit, but the 68HC11 required a different configuration: 1 start bit, 8 data bits, and 1 stop bit.

The data coming from the microprocessor is made up of two ASCII characters that represent one byte. In order to be able to use this data, they had to be changed into the 16-bit integers which the combination of ASCII characters represented.

5.3.2 68HC11 EVB Communication Software

While the host computer is performing other tasks, the 68HC11 will sit and wait until some information is requested from the host computer. As soon as this happens, it will immediately start performing the desired task. Delimiters, indicating the start and end of the transmission, are implemented so the host can verify that the microprocessor has acknowledged the request for a specific task.

5.4 Software Developed to Control the Tactile Sensor

In order to write the software to control the tactile sensor, it was first necessary to decide which tasks were going to be performed by the microprocessor and which tasks were the host's responsibility. As is mentioned throughout this thesis, one of the main objectives was to speed up the original tactile sensor by performing the least number of operations in the microprocessor. Having this in mind, I decided to use the microprocessor to

perform the data acquisition, and leave the data manipulation to the host computer.

5.4.1 Software Developed for the 68HC11

5.4.1.1 Sensor Commands

The software developed to control the data acquisition, from the 68HC11 side, has a similar functionality as the one used in the old sensor design. Out of all the options offered in that software, there were only two commands that applied to the redesigned sensor. These two commands are: tacScanAll, and tacElementOne.

5.4.1.1.1 tacScanAll Command

The tacScanAll command polls each one of the 160 sites and gets the state of the sensor. This command is useful due to the non-uniformity of the readings at each one of the sites. Deformation, temperature, continued use, aging, etc. causes the zero force voltage at each one of the sites to fluctuate. Therefore, before any force is applied to the sensor pad, this command must be invoked. Also immediately after the force is applied, this command should be call again to find out the nature of the pressure applied.

There are two arguments for this function: the first one is a pointer to a software array of size 160 where the state of the sensor will be stored. The second argument is the I/O port used on the host computer.

5.4.1.1.2 tacElementOne Command

This command is used whenever there is a need to explore the force applied to only one point of the tactile sensor. Before this command is invoked and before any pressure is exerted on the sensor pad, the tacScanAll command must be called to get the current state of the sensor before any force is applied.

There are five arguments that have to be defined when this function is call. The first two arguments are two characters that correspond to the hexadecimal number that activates the desired diode. The third and fourth arguments correspond to the transistor that is going to be activated. The last argument corresponds to the I/O port used by the host computer. This function returns the state of the sensor at the chosen point.

5.4.1.2 A/D Converter Operation

There were two choices as how the A/D could be configured. In the first choice, the selected channel is converted 4 consecutive times with the first result being stored in A/D result register 1 (ADR1) and the fourth result being stored in register ADR4. After the fourth convertion is complete, all the convertion activity is halted until the user decides to continue the process. In the second choice, instead of stopping on the fourth convertion, the converter continues convertion storing the fifth convertion in register ADR1, the sixth convertion in register ADR2, and so on. Based on this I decided to configure the A/D to operate in the first described manner.

For each one of the sites, this convertion process is repeated twice to be able to average 8 sampled readings.

5.4.2 Software Developed for the Host Computer

Upon reaching the host, the data is converted from an ASCII representation to an integer representation. Now the data is in the form of a voltage, and ranges from 0V to 5V.

The first hexadecimal character corresponds to the left nibble of a byte, and the second corresponds to right nibble of the byte. Using Table 5.1, the two hex characters can be combined and translated into a voltage ranging from 0 V to 5V.

Table 5.1 Analog Input to 8-Bit Result Translation Table

	bit 7	bit 6	bit 5	bit 4	bit 3	bit 2	bit 1	bit 0
% [1]	50%	25%	12.5%	6.25%	3.12%	1.56%	0.78%	0.79%
Volts [2]	2.5	1.25	0.625	0.3125	0.1562	0.0781	0.0391	0.0195

(1) % of VRH - VRL

(2) Volts for VRL = 0 V; VRH = 5.0 V

5.5 Data Acquisition Example

In order to verify that the previously described software works, a simple data acquisition program was written. In order to ensure best operation of the tactile sensor, a 20 minutes warm-up period after power-up is necessary. Before any pressure was applied to the sensor pad, the tacScanAll command was executed to obtained the state of the pad while it was unloaded. Then, the program was executed again but now applying pressure to the pad. Several runs of the experiment were performed but only one of them is shown. In the case shown, a two forces are applied to the sensor pad.

The data gathered from the programs was converted into a Matlab file and then plotted. Two kinds of plots were obtained for each experiment, a mesh plot and a contour plot. The mesh plots used as x and y points the position of a site in the sensor, whereas z corresponds to the voltage at that particular point. The contour plots show with more clarity where the pressures are being applied in the sensor. In Figures 5.1 and 5.2, a contour plot and a mesh plot, show the state of the sensor before any pressure is applied to it. Figures 5.3 and 5.4 are plotted after pressure is applied to the pad in the indicated fashion.

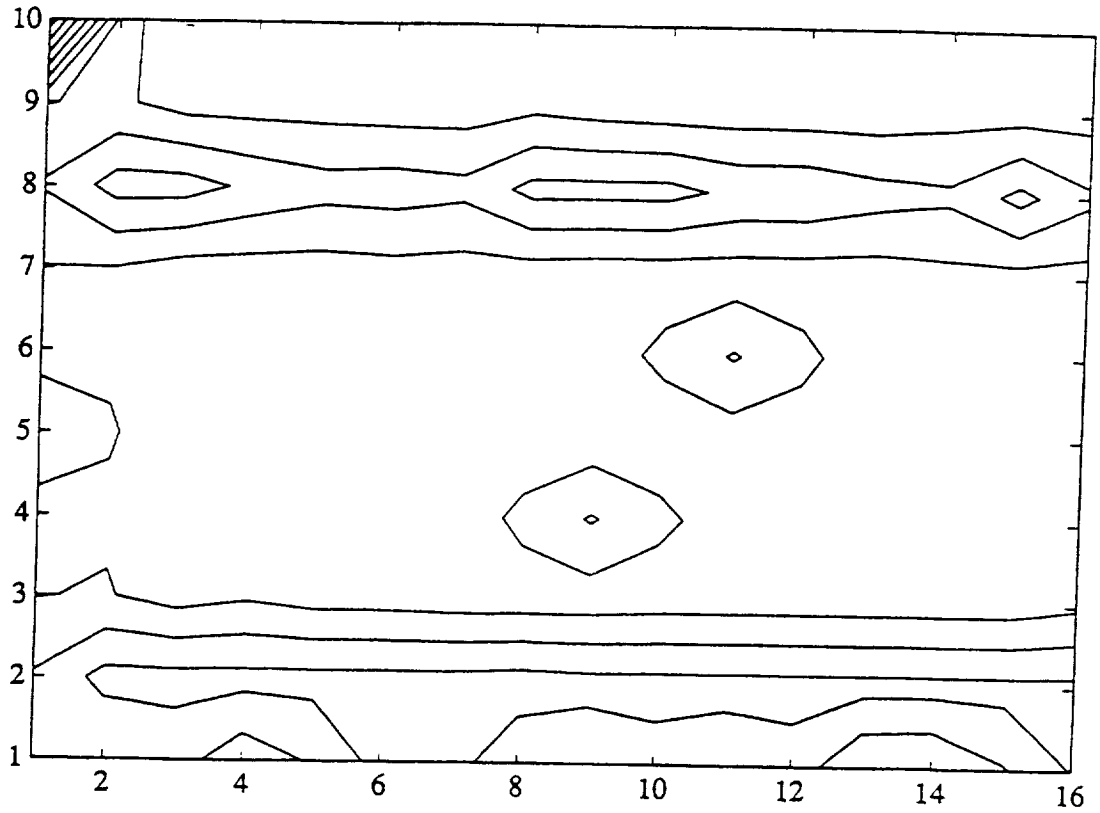

Figure 5.2 Contour Plot of the Sensor Pad Before a Circular Force is Applied.

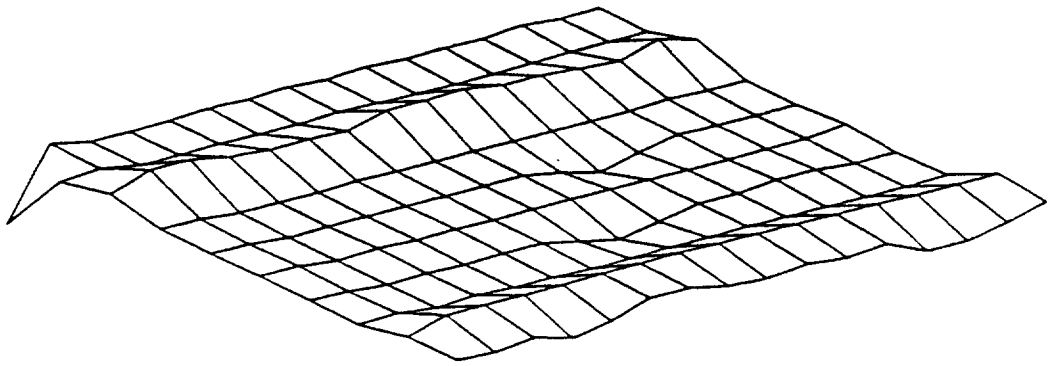

Figure 5.3 Mesh Plot of the Sensor Pad Before a Circular Force is Applied.

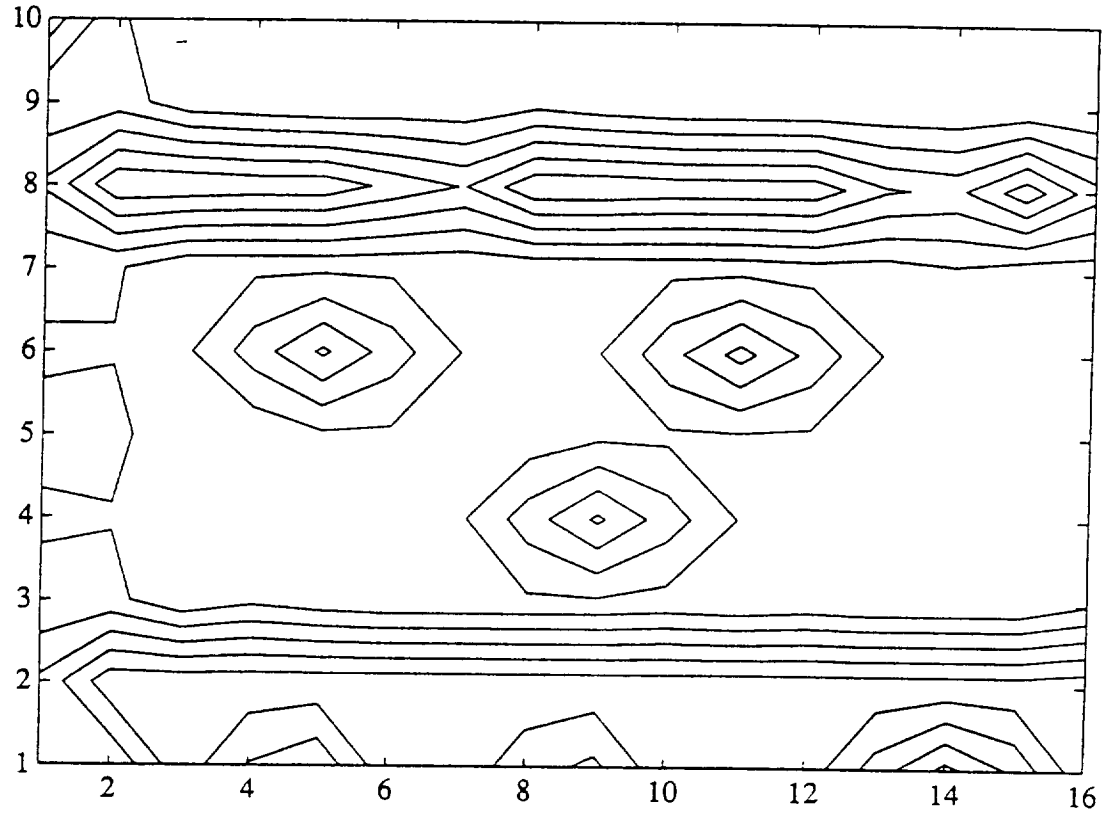

Figure 5.4 Contour Plot of the Sensor Pad After a Circular Force is Applied.

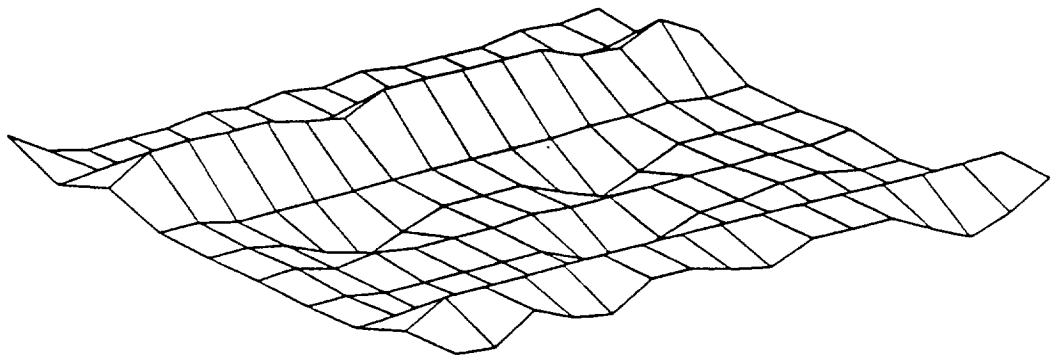

Figure 5.5 Mesh Plot of the Sensor Pad After a Circular Force is Applied.

CHAPTER 6

DISCUSSION

The improvement of a tactile sensor array made by Lord Corporation was the main objective of this research. This objective meant speeding up the sensor's response time, and redesigning its interface so the sensor could be controlled from any workstation. In order to accomplish this task, several steps were taken: first, an understanding of the tactile sensor hardware was needed. After this, exploratory work on the behavior and characteristics of the tactile sensor was performed. When enough information about the sensor was achieved, its old microprocessor, a 6502, was replaced with a 68HC11 EVB. Finally, control software was developed in order imitate some relevant functions of the old tactile sensor.

As it was mentioned in Chapter 2, the behavior of the tactile sensor hardware was studied and specifications for the analog board, belonging to the original tactile sensor, were produced. It was also decided at this stage that this analog board would remain as part of the modified tactile sensor. The other board, which contained the digital circuitry, was discarded as the 68HC11 EVB took the place of the controlling microprocessor. At this time, an issue which was taken care of in the original digital board, was addressed: the restriction in the output range and its accuracy.

After studying the manipulation done by the tactile sensor board on the output signal, I decided to design the final stage of amplification to the signal. This final stage involved the mapping of a signal ranging from +12V to -12V to a range between 0V to 5V. The 0V to 5V range was needed in

order to use the A/D converter inside the 68HC11, and the voltage map circuitry implementation shown in Chapter 4 performed this task.

Extensive research on the behavior of the tactile sensor pad was performed. The experiments were simple, but important enough so that relevant information about the characteristics of this tactile pad could be gathered. The tactile pad is made of a type of elastomeric material, which according to some literature has a very low hysteresis [6]. The first set of experiments done to the pad had as a goal to map, in an accurate fashion, the output voltage from the tactile sensor to a useful type of measurement, a force reading. After it was established that the desired output was a force in the z direction (force perpendicular to the pad surface), several readings throughout the pad were taken using the setup previously described in Chapter 3. The results were plotted, and a linear regression analysis for these points was conducted. The results of the regression analysis for several points in the array were compared. At this point, I had to decide in what neighborhood of applied forces I desired a better mapping. After a careful consideration, I decided that most of the pressures exerted on the surface will not be extremely large. Therefore, I strived for better mapping at lower forces.

The second set of experiments performed on the tactile pad had the goal of finding the precision of the voltage readings coming from the sensor pad. In order to obtain the answer to this question, hysteresis experiments were conducted on the pad. As you may gather from the plots explained previously in Chapter 3, the claim by some authors that the elastomeric pad on this sensor had a very low hysteresis is not true [3]. According to the hysteresis plots shown in Chapter 3, any force reading from the sensor will

not be very accurate. Nevertheless, in the linear region, where force readings are matched to the expected force readings, the effects of hysteresis are considerable but tolerable.

The topic of this sensor pad sensitivity was the subject of the third set of experiments. At this stage it was proven that the tactile pad is very accurate within a ±1.56% margin of error. It was noticed that there is also some error introduced by the A/D when the conversion takes places. This problem can be seen in places where no force is applied. When the data for the unloaded sensor is subtracted from the data for the loaded sensor, at some places there is a discrepancy of 0.0195 V. This error is consistent with these error that this A/D converter is expected to give.

The other problem noticed at this point is probably due to some malfunction of the diode-transistor pairs (1,1) and (17,19). There is voltage drop recorded at this point when in reality no force is applied. The solution for this problem is probably to compensate the reading at this places by means of software.

The final set of experiments performed to the pad had to do with the influence caused to the neighbors where a force is applied to a site. By doing this experiment, the maximum force that could be applied to a point before damage occurs could be derived. After choosing a couple of points and watching the behavior of the neighboring sites, I concluded that as long as the force is less than 0.857 Newtons, no voltage readings on the neighbors would be recorded. This is a good characteristic of this pad because, if the sensor is used in an application where a binary response is needed and this response has to be in real-time, it could be quickly deciphered whether an object is

present or not. All of the previously described experiments were conducted using a force applied to one point, instead of the whole sensor pad.

The previously described experiments were performed at the hardware level, using a voltmeter and logic probes instead of using software. The reason for this decision was simple; developing software to calibrate the tactile sensor would have meant putting all the necessary hardware together, and then if problems arose, to try and figure out if it was the hardware's fault or the software's fault. In my approach, after gaining knowledge of the workings of the old tactile sensor, I put together a test board where I would manually select each point of the array and study its characteristics. By doing this, my theories about how the board worked were confirmed, and the necessary steps to study the behavior of the board were simpler. Then, after the hardware was fully understood and the investigation about the behavior of the tactile sensor was enough for this project's scope, I felt it was appropriate to move on to the next stage, the interface between the analog board with the 68HC11 board, and the development of control software.

The only issues that arose when the tactile sensor board was interfaced to the 68HC11 evaluation board were which ports to use and what was the desired function of the A/D converter. I chose ports B and C as the controlling ports of the multiplexers. The input coming from the sensor was fed into port E, the A/D port input. There were two choices as how to configure the A/D. The A/D could convert the input signals continuously or convert four readings and then stop. I chose the latter scheme because in this one I would know for certain that the sampled voltages are from the current site instead of belonging to the previous site.

The last stage of this project consisted of developing the software to communicate and control the tactile sensor. A couple of problems arose at this part; the Sun workstation is normally configured with 7 data bits while the 68HC11 only accepts 8 or 9 data bits. As a result, the configuration of the workstation had to be changed and, if any other workstations are going use to control the sensor, it should be kept in mind that a reconfiguration of the I/O port is needed. The only thing needed is a small function that is called at the beginning of the program (supplied with the library).

The second problem encountered had to do with properly configuring the 68HC11. At power-up, the default I/O port is the ACIA in the 68HC11. For this project's purposes, there was a need to use the SCI port, thereby a special configuration was needed. In order to enable this port, a logic one has to be written to any address from $4000-$5FFF.

The previous paragraphs give a description of all the issues addressed during the course of my thesis. In the next section, the conclusions of this research will be presented, and suggestions for further improvements on the tactile sensor will be given.

CHAPTER 7

CONCLUSIONS

A tactile sensor made by Lord Corporation was the subject of this research. One of the problems of the old sensor was its speed. I tried to make the new design faster by just performing the data acquisition in the microprocessor, and leaving the manipulation of data to the host computer. Another problem with this sensor was its lack of precision. After some study of the hardware, I reached the conclusion that in order for the design to be simpler, the designers at Lord Corporation sacrificed the sensor's precision. Finally, the A/D converter used in the old design had a data width of 4 bits which would result in a large error after the digital conversion. In my design, the 8-bit A/D supplied with the 68HC11 was used, introducing less error in the digital conversion.

There is still room for improvement for this sensor. Some possible suggestions are: adding another digital gain chip that could make the sensor even more sensitive, and using a different A/D that could accept voltage ranges from -12 V to +12V so that the errors introduced by mapping this range into 0V to 5V are eliminated.

This modified tactile sensor will yield better results in binary applications where there is a need to know only whether there is an object present and where. The error in this type of operation is small, 1.56%. In applications where an applied force is needed, the formula described in Chapter 3 can be used. This formula will probably not yield extremely

accurate results, but it will provide the user with a good notion of the magnitude of the applied force.

LITERATURE CITED

[1] Dario, P., Bergamasco, M. and Fiorillo, A.S., *Force and Tactile Sensing for Robots*, Springer-Verlang, New York, NY, 1988.

[2] Bergej, Stefan, "Planar and Finger-shaped Optical Tactile Sensors for Robotic Applications," *IEEE Journal of Robotics and Automation*, Vol.4, No.5, pp. 472- 484, October 1988.

[3] *Preliminary LTS-200 Operations Manual*, Rev 0.7, Lord Corporation, Cary, NC, 1984.

[4] Sekelsky, Stephen M., *The Usefulness of the LTS-200 Tactile Sensor*, Senior Project Final Report, ECSE, July 1989.

[6] Motorola Inc, *M68HC11EVB Evaluation Board User's Manual*, 1986.

[5] Rebman, J. and Morris, K.A., *A Tactile Sensor with Electrooptical Transduction*, Springer-Verlag, New York, NY, 1987.

BIBLIOGRAPHY

Allen, Peter K., *Robotic Object Recognition Using Vision and Touch*, Kluwer Academic Publishers, Norwell, MA, 1987.

Colley, William C., *68HC11 Cross-Assembler (Portable) Version 0.1*, 1987.

Lipovski, G.J., *Single and Multiple-Chip Microcomputer Interfacing*, Prentice-Hall Inc., Englewood Cliffs, New Jersey, 1988.

Luo, Ren C. and Kay, Michael G., "Multisensor Integration and Fusion in Intelligent Systems," *IEEE Transactions on Systems, Man, and Cybernetics*, Vol.19, No.5, pp. 901-931, September/October 1989.

Mazda, F.F, *Electronic Engineer's Reference Book, 5th Edition*, Butterworths, London, England, 1986.

Motorola Inc, *M68HC11 Reference Manual*, Prentice-Hall Inc, Englewood Cliffs, New Jersey, 1989.

Ritchie, Dennis M and Kernighan, Brian K., *The C Programming Language*, Prentice-Hall Software Series, Englewood Cliffs, New Jersey, 1978.

Roach, John W., Paripati, Praveen K. and Wade, Michael, "Model-based Object Recognition Using a Large-Field Passive Tactile Sensor," *IEEE Transactions on Systems, Man, and Cybernetics*, Vol. 19, No. 4, pp. 846-853, July/August 1989.

Tsai, Jodi, *M68HC11 Gripper Controller Software* , Master's Thesis, May 1991, ECSE, Rensselaer Polytechnic Institute.